Three Phase Induction Motor Drive: A Systematic Review on Dynamic Modeling, Parameter Estimation, and Control Schemes

Usha Sengamalai [1], Geetha Anbazhagan [1], T. M. Thamizh Thentral [1], Pradeep Vishnuram [1], Tahir Khurshaid [2,*] and Salah Kamel [3]

1   Department of EEE, SRM Institute of Science and Technology, Kattankulathur, Chennai 603203, India
2   Electrical Engineering Department, Yeungnam University, Gyeongsan 38541, Korea
3   Electrical Engineering Department, Faculty of Engineering, Aswan University, Aswan 81542, Egypt
*   Correspondence: tahir@ynu.ac.kr

Abstract: An induction motor is generally used in industrial applications because it is reliable, robust, and low cost. Reliability is one of the essential parameters based on which the motor is selected, and the induction motor primarily comes into force. The well-founded induction motor gives good results under various operating states. To achieve this, the values of the motor are kept in mind. Dynamic simulation plays a significant part in evaluating the model's design process to eliminate design errors in typical construction types and when testing the motor drive system. The induction motor is modeled in a synchronously revolving rotor flux-oriented frame, which is used as a reference. For sensorless vector control and induction motor control methods, accurate knowledge of a few induction motor parameters is necessary. The presentation of the drive will degrade if the original data in the motor do not match the values utilized in the controller. Various mechanisms have been developed to calculate the online and offline parameters of the induction machine for its application in high-performance drives. The foremost grail of this review paper is to present dynamic modeling and other considerable approaches used for estimating the induction motor parameter. This paper also constitutes some simulation examples related to dynamic modeling and parameter estimation techniques, which may be useful for specialists in the field of electric drive control systems.

Keywords: induction motor; parameter estimation; dynamic modeling; observer; model reference adaptive system (MRAS); intelligent technique

1. Introduction

The most common type of motor used in industries is the induction motor because of its reliability, robustness, and low cost. The DC motor was used initially, as it offers controlled speed and torque. However, due to the existence of a commutator, it requires constant maintenance. This problem was overcome by using an induction motor with no commutator. The elimination of the commutator in an induction motor is lower in cost and broader in its application. The main problem with an induction motor is its speed control, which is arduous. Advancements soon rectified this problem in power electronic converters. Now to control the speed of the motor, inverters were being used. Using an inverter eliminated the speed control problem, which led to another problem related to stability in an inverter-fed induction motor.

In order to carry out the analysis of an asynchronous motor, the induction motor is modeled in a frame that revolves synchronously and is flux-oriented. For sensorless vector control and the control schemes of the induction motor, excellent skills are required for at least some of the data of an asynchronous motor. So, the estimation of parameters needed to be taken care of. Due to the extensive use of induction motors across various industrial sectors, simulation and dynamic modeling of induction motors are significant to

both businesses and academia. An induction motor's dynamic and steady-state analyses are challenging. The advantage of dynamic modeling is that it aids in understanding asynchronous motor behavior in dynamic mode. The mechanical equations used in dynamic modeling include speed, torque, and time. Dynamic modeling can also be used to simulate the differential voltages, flux links, and currents between the static stator and rotating rotor. Typically, an inverter with a speed sensor drives an induction motor. However, this speed sensor has the potential to reduce system reliability and raise investment costs. Its implementation is challenging as well. Several studies use induction motors with speed sensorless drives to overcome this challenge. Different speed estimators were taken into consideration under the absence of feedback, and their performance was compared when internal parameter change and outside disturbances were present. The MRAS staging was found to be superior to the variant speed estimator. The fact that MRAS requires a detailed model of the drive system and the speed differential between the two motors, however, added to its drawback. The system cannot attain total stability if there are significant speed variances between the two motors [1,2]. In light of this, a novel sensor-free device based on an adaptive observer and a modified decoupling-controlled technology was presented. However, due to the speed estimation being unsteady in the regenerative zone, this technology was not very practical [3].

This research utilizes reduced-order observers to analyze the speed and flux assessments of asynchronous motors without sensors [4–6]. There are no gain options that do not offer stability. This study also discusses some recently discovered reduced-order observer features in addition to the aforementioned. The authors work on a technique termed vector control for two induction motors operating in parallel. This approach, which is based on system parameter averages and differences, calls for high-speed digital processors [7,8]. The analysis of a single inverted-fed multiple-asynchronous motor operating in parallel is given based on the approach of the Laplace transform of the output to the Laplace transform of the input model. It came to the conclusion that the system was unable to achieve stability under strongly loaded conditions and could only maintain stability under unequal load conditions [9,10]. The performance of high-power asynchronous motors is examined using the constant voltage by a frequency closed loop approach without sensors based on space vector pulse width modulation (SVPWM) [11–13]. It has been suggested to use a DC-to-AC converter with a DC link to drive an induction motor. The SVPWM approach aids in lowering secondary switch losses and current values. Given that the commutation circuit is active for a considerable amount of time, it is crucial to reduce losses and current values at the secondary switch [14].

The control of the switches is obtained by soft and hard switching methods with increased efficiency. Four auxiliary switches are used in order to obtain fast transients as compared to power switches. Induction motor is controlled by a quasi-resonant inverter using a direct torque control scheme with space vector modulation. The source voltage is clamped with DC link [15]. A soft switching technique is employed to manage the voltage, torque, and speed [16,17]. Induction motor monitoring is the process of identifying a motor's developing defects. An induction motor experiences issues such as over voltage, above-rated current, high temperature, high-rated speed, monitoring of vibration, etc., while it is in operation. It is crucial to establish awareness of a motor drive system's fault mode reaction from the perspectives of enhanced system design, sanctuary, and fault impartial control [18,19].

The evolution of induction motors from being a stable speed motor to an unpredictable speed motor and torque machine has been observed over the past few decades. However, the problem of controlling a DC motor during fault conditions [20] remained a challenge to its growth. An intrinsic and challenging topic for electrical researchers was the behavioral study of induction motors during abnormal conditions when faults are present and its diagnosis (fault diagnosis). In an industrial plant, a sudden unexpected breakdown of an induction motor due to faults can be disruptive to the high level of production process. To increase the quality and reliability and to lower the cost of production, a programmable logic

controller (PLC) is being employed in many industries to carry out the automation process. PLC controlled protective relay handle failures such as phase loss, above-rated current, above-rated voltage, without unequal phase displacement of supply voltage, without unequal phase displacement of currents, and the uncontrolled repeated starting [21,22].

The rotor faults and the stator faults are the two types of faults existing in electrical motors. The most common of these faults is the stator fault. Inter-turn short circuit in one of the stator coils is the main cause ofthe origin of this type of fault. This short circuit leads to increased heating that eventually leads to ground faults and finally the breakdown of the stator takes place. Rotor faults contribute to only 20% of the overall faults in induction motors, yet fault detection diagnosis of rotor faults is important for industrial applications [23]. High current flow in adjacent bars of an induction motor happens because of broken rotor bars and air gap eccentricity. This eventually leads to further potential breakage and stator faults as well. In order to diagnose and rectify problems related to broken rotor bar and air gap eccentricity, MCSA (motor current signature analysis) is widely used in industries [24].By applying the predicted parameters, the induction motors are designed dynamically. Thus, the working method target to develop its efficacy from the designed grip for propulsion by using a multilevel inverter in place of the existing voltage source inverter thereby diminishes the torque ripple and speed deviation under the parameter variations. The system requires better control performance, precision and quicker torque response and they were very difficult because of computing. The speed of the motors can be sensed by using the generators called Tacho-generators or encoders. This will boost up the entire expenses. Moreover, advanced technology has been developed to drive the motors without the use of speed sensors.

The parameter estimation of an induction motor by a no-load test, resistance test in DC, and a blocked rotor test is analyzed in a simulation as well as hardware setup. The dynamic modeling of an induction motor with estimated parameters is proposed in this paper. The performance investigation of induction motor drive in parallel with field-oriented control using the MRAS technique with speed controller is reviewed.

Industries frequently employ variable speed drives (VSDs) to link induction motors to the main supply. However, the use of VSDs frequently results in current ripple, making it challenging to locate the fault [25]. Discrete wavelet transform was used to obtain the various stator current harmonics. The benefit of local representation of the current signal for both healthy and malfunctioning modules is provided by DWT. Additionally, using a proportional integral (PI) controller to control KP and Ki values produces changeable data. The speed control of the induction motor is illustrated in Figure 1.To identify faults in induction motors, numerous techniques such as short-time Fourier transform, Gabor transform, wavelet transform and fast Fourier transform are used. Out of all the above-mentioned techniques, the fast Fourier transform is the easiest to implement. The only disadvantage of this technique is that transient signals using the time frequency representation cannot be analyzed by it.

On the other hand, STFT (short-time Fourier transform) is useful for analyzing short-lived signals using time frequency description, but its drawback is that it can only examine the signal with all frequencies for a stable-sized window. This marshal to imperfect frequency solution of this technique is that transient signal using the time frequency [26]. However, a powerful tool that helps in fault detection and diagnosis of motors by utilizing an adjustable-sized window is Wavelet Transform. The various software techniques and those used for fault diagnosis are Matlab, LabVIEW, Pscad, Neutral Net, etc. Artificial neural network, Fuzzy logic, and Space vector modulation are the several intelligent techniques that have been developed to detect the faults and early onset as well as avoid serious problems [27]. However, out of all the above-mentioned techniques, wavelet transform utilizing an adjustable-sized window is the very powerful tool used in the fault detection of induction motor. Furthermore, the structure of this article is as follows: Section 2 presents the modeling and result analysis of a three-phase induction motor; Section 3 explicates the simulation and result discussion of three-phase induction motor dynamic

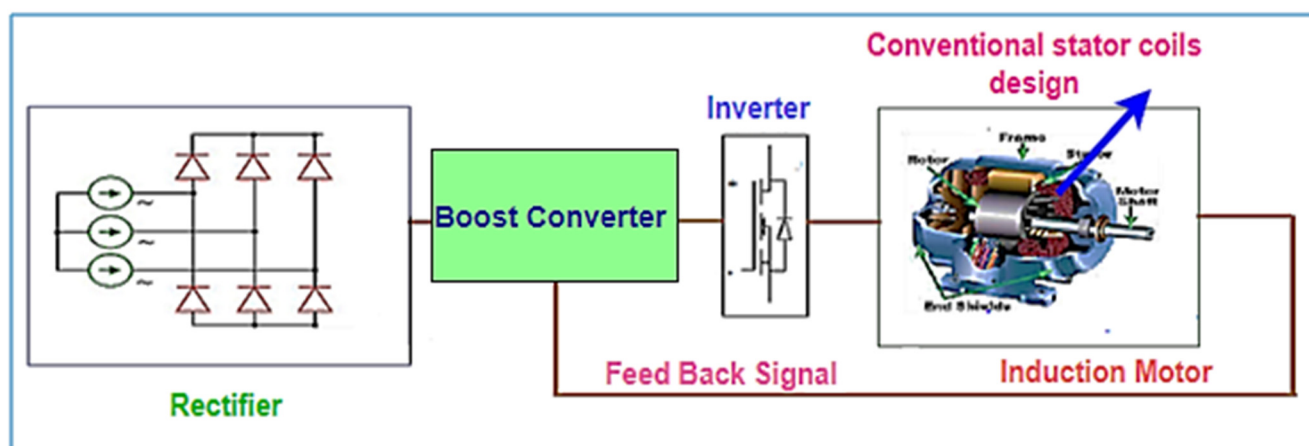modeling; Section 4 emphasizes the hardware results and discussions; and Section 5 draws the conclusion.

Figure 1. Controlling technique of motor drive.

2. Modeling and Result Analysis of Three-Phase Induction Motor

Accurate induction motor modeling is essential for building the machines' controllers and for spotting problems with the machines. Any characteristics, including flux, torque, and speed, are based on the controller's design, which is itself based on the transfer function. First-principle methods, system identification techniques, the finite element method, the equivalent magnetic circuit approach, the use of ordinary differential equations, linear/nonlinear differential equations, models with lumped parameters and distorted parameters, static and dynamic modeling, and others are the various types of mathematical modeling. The theory of electrical machines uses the mathematical representation provided by ordinary differential equations.

The interaction between electromagnetic torque and the primary electrical and mechanical parameters is represented by them. Partial differential equations can be utilized to more thoroughly characterize the electrical machines' magnetic fields, temperature distributions, and other quantities. However, the disadvantage of employing partial differential equations for research is that they are quite difficult to understand. Simulation and dynamical modeling of induction motors are crucial for both academic and business purposes. Because induction motor drives are so common in many building contexts and for induction motors with sensorless control, its value is increasing. Therefore, a thorough explanation of the dynamic modeling of an asynchronous motor is presented in this study.

2.1. Dynamic Modeling of Three-Phase Induction Motor

Since induction motor drives can be used in various industrial environments, the simulation and dynamic modeling of induction motors are critical to both businesses and academia. Therefore, mathematical modeling is prepared to carry out the analysis. Induction machine modeling has constantly been attracting research, as these machines have various operations models and are used in large numbers. The reference frame theory has been efficiently analyzed as a potent approach to determining the mathematical model of the three-phase induction motor. The value of dynamic modeling aids in understanding motor behavior in dynamic mode. D-Q modeling of an induction motor is modeled by three different reference frames, as shown in Figure 2 [28,29].

Mechanical equations involving speed, torque, and time are included in the dynamic modeling. Dynamic modeling can also be used to simulate the differential voltages, flux links, and currents between the fixed stator and rotating rotor. Any rotating reference frame, stator reference frame, or rotor reference frame can be reported uniquely for an induction motor. It is generally more favorable to simulate an asynchronous motor in a

stationary reference frame while proceeding with the transient studies of an adjustable speed drive. This reference frame offers less complex calculations because it has zero frame speed. A synchronously rotating frame is used to carry out small signal stability analysis under the same operating condition. This yield was used to carry out the small signal stability analysis and the same operating condition. This yield is used for the enduring value of steady-state voltage and current under identical loaded conditions [30,31].
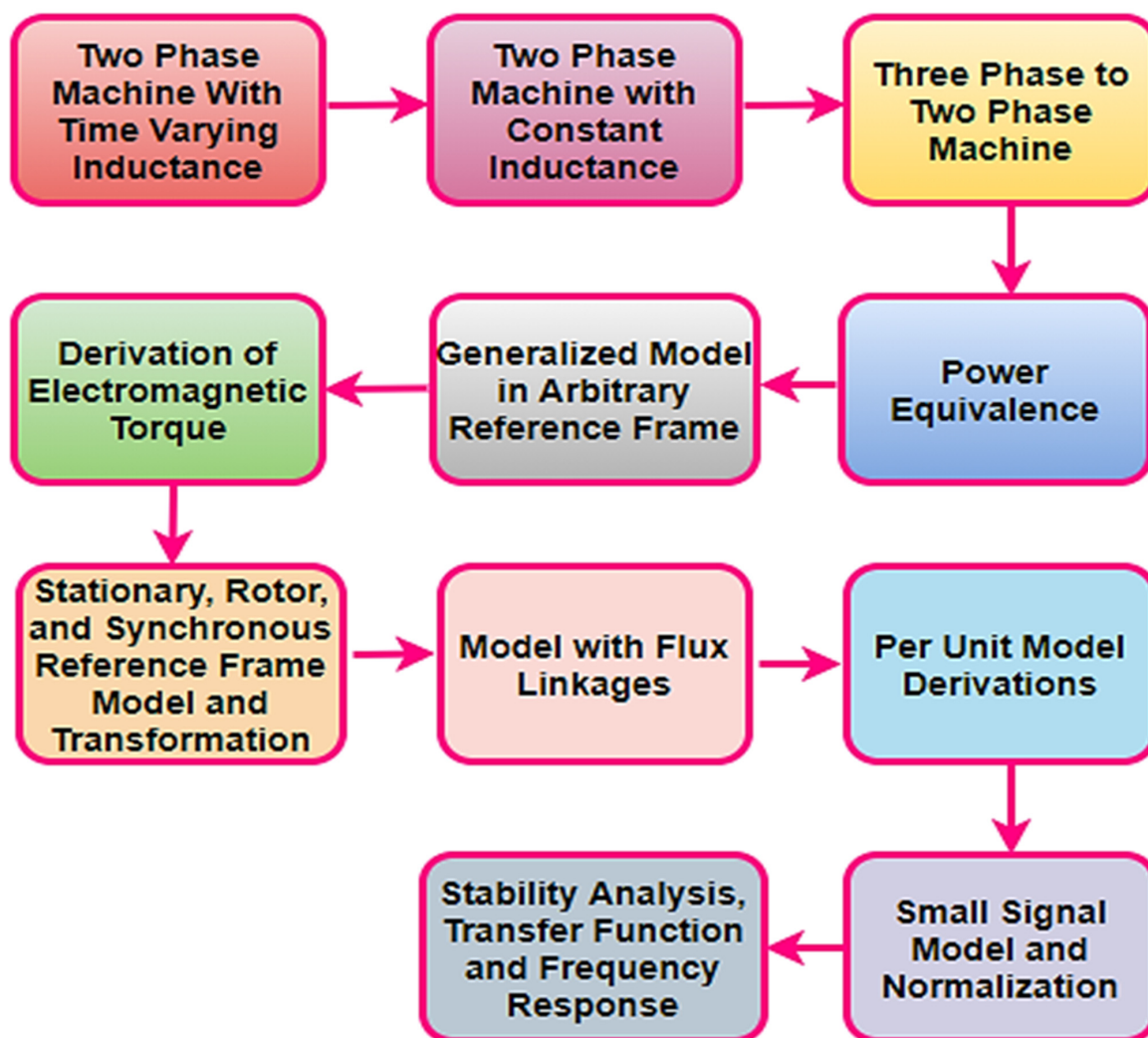

Figure 2. Three-phase induction motor dynamic modeling.

Time-dependentinductances in two-phase machinery: The inductances linking the primary and secondary turns are an outcome of the second position, theta r. They are imagining being sinusoidal due to the reason for sinusoidal MMF dispensations in the windings. Hence, they keep varying with time as rotor position varies with time and therefore leading to time-varying inductances

Constant inductances in two-phase machinery: To obtain inductances, the actual rotor must be replaced with the fictitious rotor on the d and q axes. In this way, the fictitious rotor produces the same MMF as it has an equal number of windings for all phases as the actual rotor turns. In the instance of changing the speed of the rotor and if its variations are independent of the current, then the system of equation will become nonlinear.

Three-phase to two-phase transformation: The uniformity of the three-phase inductance machine and two-phase induction machine must be established. This equivalence must be dependent on the fairness of the MMF processed through two- and three-phase windings and identical current magnitude.

Power equivalence: To obtain definitive explanations in the modeling investigations and simulation, the input power to the three-phase motor must be equal to the two-phase machine. The model development has kept the d and q axes stationary concerning the stator in the power equivalence equations. These axis or frames are known as reference frames.

Generalized induction machine models in arbitrary reference: Transformation is the procedure of changing one set of volatiles by another type of volatile. To ease the solution of the laborious equations with time fluctuate coefficients or to introduce all the variables in a general reference frame, transformation is used. The essential feature of transformation, which rationalizes its high vogue, is that it eliminates the time-changing inductance from the potential difference between two points and current equations.

Electromagnetic Torque: The torque is obtained from the machine calculations by considering the input power and its various elements, such as resistive losses, power, rate of change of stored magnetic energy and power from the reference frame. The above-mentioned magnetic energy needs to be zero, as there is no power element due to the presentations of the reference frame. However, it is not true dynamically. Depending on these examinations, electromagnetic torque is made.

In the electromagnetic torques equation, p is the number of poles, L_m describes the magnetizing inductance, and i_{qs} and i_{ds} are the stator currents in the d and q axes, respectively. Finally, i_{dr} and i_{qr} are the rotor currents in the d and q axes. The equation of flux linkage helps in the depletion of several complex terms in the d-q equations, which fetch their solutions by manipulating the analog and cross-computers. The best feature about this is that even when the voltage and current are intermittent, the flux linkages are sustained.

2.2. Mathematical Modeling of Three-Phase Induction Motor in Reference Frames

Induction motors are the motors generally used in industries these days. During the starting up of induction motors, it tends to draw large currents at times and produces voltage immersion and ripple torques. Induction motors gain their full speed within a fraction of a second, precisely 0.2 s, with its electrical torque exhibiting 50 Hz oscillations. If self-control is not considered, the motor starting current gets as high as 9.5 p.u. In such a case, the d-q unpredictable in the frame of reference tends to differ, although the performance of the manual variables as estimated by each reference frame is uniform. The difference in the d-q variables can be rectified by adequately matching the reference frames. Several methods have been developed for this, and the d-q or two-axis transforms are the best suited and most accurate. Three preferred speeds/frames of reference exist: the stationary reference frame, the synchronously rotating reference frame, and the rotor reference frame [32].

The arbitrary reference frame of a generalized model is derived from the following equations [32].

$$\begin{bmatrix} i_{qs} \\ i_{ds} \end{bmatrix} = \begin{bmatrix} \cos\theta_c & \sin\theta_c \\ -\sin\theta_c & \cos\theta_c \end{bmatrix} \begin{bmatrix} i_{qs}{}^c \\ i_{ds}{}^c \end{bmatrix}$$
$$\begin{bmatrix} i_{qs}{}^c \\ i_{ds}{}^c \end{bmatrix} = \begin{bmatrix} \cos\theta_c & -\sin\theta_c \\ \sin\theta_c & \cos\theta_c \end{bmatrix} \begin{bmatrix} i_{qs} \\ i_{ds} \end{bmatrix} \tag{1}$$

$$\begin{bmatrix} v_{qs} \\ v_{ds} \end{bmatrix} = \begin{bmatrix} \cos\theta_c & \sin\theta_c \\ -\sin\theta_c & \cos\theta_c \end{bmatrix} \begin{bmatrix} v_{qs}{}^c \\ v_{ds}{}^c \end{bmatrix}$$
$$\begin{bmatrix} v_{qs}{}^c \\ v_{ds}{}^c \end{bmatrix} = \begin{bmatrix} \cos\theta_c & -\sin\theta_c \\ \sin\theta_c & \cos\theta_c \end{bmatrix} \begin{bmatrix} v_{qs} \\ v_{ds} \end{bmatrix} \tag{2}$$

From the above matrix

$$v_{qs}{}^c = v_{qs}\cos\theta_c - v_{ds}\sin\theta_c$$
$$v_{ds}{}^c = v_{ds}\cos\theta_c + v_{qs}\sin\theta_c \tag{3}$$

$$i_{qs}{}^c = i_{qs}\cos\theta_c - i_{ds}\sin\theta_c$$
$$i_{ds}{}^c = i_{ds}\cos\theta_c + i_{qs}\sin\theta_c \tag{4}$$

From the general equation of induction motor

$$v_{qs} = (R_s + L_s p)i_{qs} + L_m p i_{qr} \\ v_{ds} = (R_s + L_s p)i_{ds} + L_m p i_{dr} \tag{5}$$

$$v_{qr} = (R_r + L_r p)i_{qr} + L_m p i_{qs} \\ - L_m \omega_r i_{ds} - L_r \omega_r i_{dr} \tag{6}$$

$$v_{dr} = (R_r + L_r p)i_{dr} + L_m p i_{ds} \\ + L_m \omega_r i_{qs} + L_r \omega_r i_{qr} \tag{7}$$

Substitute $v_{qs}, v_{ds}, v_{qr}, v_{dr}$ in the above equations; the arbitrary reference generalized model is given by

$$\begin{bmatrix} V_{qs}^c \\ V_{ds}^c \\ V_{qr}^c \\ V_{dr}^c \end{bmatrix} = \begin{bmatrix} R_s + L_s p & \omega_c L_s & L_m p & \omega_c L_m \\ -\omega_c L_s & R_s + L_s p & -\omega_c L_m & L_m p \\ L_m p & (\omega_c - \omega_r)L_m & R_r + L_r p & (\omega_c - \omega_r)L_r \\ -(\omega_c - \omega_r)L_m & L_m p & -(\omega_c - \omega_r)L_r & R_r + L_r p \end{bmatrix} \begin{bmatrix} i_{qs}^c \\ i_{ds}^c \\ i_{qr}^c \\ i_{dr}^c \end{bmatrix} \tag{8}$$

2.2.1. Reference Frame for Stator

It is best suited for studying the stator variables because the stator d axes are the same as a phase of stator variable. Here, reference frame speed is zero, while K represents the transformation matrix. In the reference frame of the stator, the q-axis is stable and coincides with phase a stator winding. Therefore, this reference frame is advantageous for analyzing transient development involving the stator variables. The ABC variables must be changed into d-q variables to study the electrical and mechanical behavior of the original machine correctly. This is obtainable by Park's transform. For this transformation, a zero-sequence element is introduced with the variables of d-q. This new variable handles the unbalanced voltages and inverts Park Transform. On careful observation, the voltage v_{ds} given to the stator d-axis coil is similar to the voltage of stator phase A. It was concluded that it is not inevitable to determine i_{as} individually at every step of the integration procedure by the inverse of Park's transform. This is convenient for the fixed reference frame and saves computer time [32].

Substitute $\omega_c = 0$ for the stator reference frame in the generalized arbitrary reference model [32]

$$\begin{bmatrix} V_{qs} \\ V_{ds} \\ V_{qr} \\ V_{dr} \end{bmatrix} = \begin{bmatrix} R_s + L_s p & 0 & L_m p & 0 \\ 0 & R_s + L_s p & 0 & L_m p \\ L_m p & (-\omega_r)L_m & R_r + L_r p & (-\omega_r)L_r \\ (\omega_r)L_m & L_m p & (\omega_r)L_r & R_r + L_r p \end{bmatrix} \begin{bmatrix} i_{qs} \\ i_{ds} \\ i_{qr} \\ i_{dr} \end{bmatrix} \tag{9}$$

2.2.2. Reference Frame for Rotor

It is well advanced when the investigation is confined to rotor variables, as the rotor d axes variable is similar to the rotor variables of phase a. Reference Frame speed here is equal to the rotor speed K represents the transformation matrix. In the rotor frame, the q axes of the reference frame are changing at the same speed as the winding of the rotor and are consonant with its axis. Therefore, the q-axis current and Ia status are expected to be the same [32].

Substitute $\omega_c = \omega_r$ for rotor reference frame [32].

$$\begin{bmatrix} V_{qs}^r \\ V_{ds}^r \\ V_{qr}^r \\ V_{dr}^r \end{bmatrix} = \begin{bmatrix} R_s + L_s p & \omega_r L_s & L_m p & \omega_r L_m \\ -\omega_r L_s & R_s + L_s p & -\omega_r L_m & L_m p \\ L_m p & 0 & R_r + L_r p & 0 \\ 0 & L_m p & 0 & R_r + L_r p \end{bmatrix} \begin{bmatrix} i_{qs}^r \\ i_{ds}^r \\ i_{qr}^r \\ i_{dr}^r \end{bmatrix} \tag{10}$$

This technique cannot be used in machines where both the stator and rotor are salient. The non-salient element has unequal windings; this method cannot be used for such cases. The phenomenon of brush contact, effects of commutation and surge effect cannot be entitled in this model, so they have to be handled individually. This reference frame can analyze a transient phenomenon in the rotor because the rotor d axes are unstable at slip frequency.

2.2.3. Synchronously Rotating Reference Frame

The frame is suited when the continuous signal computer is involved because both stationary and rotating d-q aggregates become steady DC aggregates. It is also convenient for analyzing several machine systems. Reference Frame speed equals the synchronous speed, and k represents the transformation matrix. The stator and rotor rotate at different speeds, while the reference frame is rotating at synchronous speed, which is relative to it. Nevertheless, the frame of reference sometimes rotates at the same speed as the rotor and stator. For such cases, this reference frame should be opted for achieving stability of controller design. The stator d axis current has a steady nature and makes the synchronous reference frame so functional when a continuous signal computer is used in analyzing simulation. Moreover, the stationary and rotating d-axis variables change steadily in this reference frame, which gives the advantage of using a more considerable integration step length for digital computers. To achieve controller stability, the linearized motor equations are to be considered. This reference frame is best suited [33].

Substitute $\omega_c = \omega_s$ for synchronously rotating reference frame

$$\begin{bmatrix} V_{qs}{}^e \\ V_{ds}{}^e \\ V_{qr}{}^e \\ V_{dr}{}^e \end{bmatrix} = \begin{bmatrix} R_s + L_s p & \omega_s L_s & L_m p & \omega_s L_m \\ -\omega_s L_s & R_s + L_s p & -\omega_s L_m & L_m p \\ L_m p & (\omega_s - \omega_r) L_m & R_r + L_r p & (\omega_s - \omega_r) L_r \\ -(\omega_s - \omega_r) L_m & L_m p & -(\omega_s - \omega_r) L_r & R_r + L_r p \end{bmatrix} \begin{bmatrix} i_{qs}{}^e \\ i_{ds}{}^e \\ i_{qr}{}^e \\ i_{dr}{}^e \end{bmatrix} \quad (11)$$

Benefits of reference frames:

(1) It reduces the number of voltage equations.
(2) The time-varying equations are converted to time-invariant ones.
(3) It reduces the complexities in voltage equations so that the performance analysis of power systems and electric machines can be conducted easily.
(4) Control algorithms needed to be represented in digital signal processor (DSP) are made easy by transformation techniques.
(5) Many of the basic techniques and interpretations, with the help of this technique, have been established concisely.

A dqo circuit of an asynchronous motor is represented in the above design as in Figures 3 and 4. This circuit consists of changing inductance, which will assist in interpreting the dynamic performance of the three-phase induction motor after simulation. The steady-state model and equivalent circuit of an asynchronous motor are advantageous in learning the machine's performance. The voltage and torque equations are time-varying and help describe the dynamic characteristics of AC motors. The complexities of these equations can be eliminated if a change in the equation is carried out such that all the time-varying inductances are measured from the equation of the machine's voltage. These time-changing inductances rise because of the relative motion of electric circuits. This is because, to deal with complex number variables in most cases, the performance of motors with space vectors becomes complicated. Control estimation is often carried out in the reference frame when asynchronous motors are supervised by the vector drive [34]. It is necessary for the frame transform to be executed in control since actual state variables are measured in a stationary frame [35–38]. The attractive transform links static frame three-phase variables to the synchronizing rotating frame of two-phase quantities. In the case where the objective is to create a rotating space vector describing a circle, three-phase sinusoidal currents are not necessary. For a circle to be described in space, two coordinates,

namely, *d* and *q* analytical geometry are required. Two coils are placed perpendicular by varying the fact, and sinusoidal current is supplied to them, displaced by an angle of 90 degrees. The two coils are called the direct coil and the quadrature coil. In the rotating frame of reference, concerning phase a, the d axis is considered, and the other axis is considered as the q axis. Thus a 3-phase system can be reduced to a 2-phase system using this method with the help of this cross-coupling between individual coils. An external advantage is that the current flowing in the coils is DC current in constant regions. The difficulties of any state value are found to be 0 in steady state by using the rotating frame of reference. In case the differentials turn out to be different from 0, they lead to a change from a steady state. Another advantage of a rotating frame of reference is that the rotor angle is known. Devising the design for presenting the phase transformation to a rotating frame of reference is yet to be figured out. Equation (12) describes the modeling and transformation of three-phase induction motors [39,40].

$$
\begin{aligned}
V_a &= \sqrt{2} V_{ms}{}^r \sin(\omega t) \\
V_b &= \sqrt{2} V_{ms}{}^r \sin\left[\omega t - \tfrac{2\pi}{3}\right] \\
V_c &= \sqrt{2} V_{ms}{}^r \sin\left[\omega t + \tfrac{2\pi}{3}\right]
\end{aligned}
\tag{12}
$$

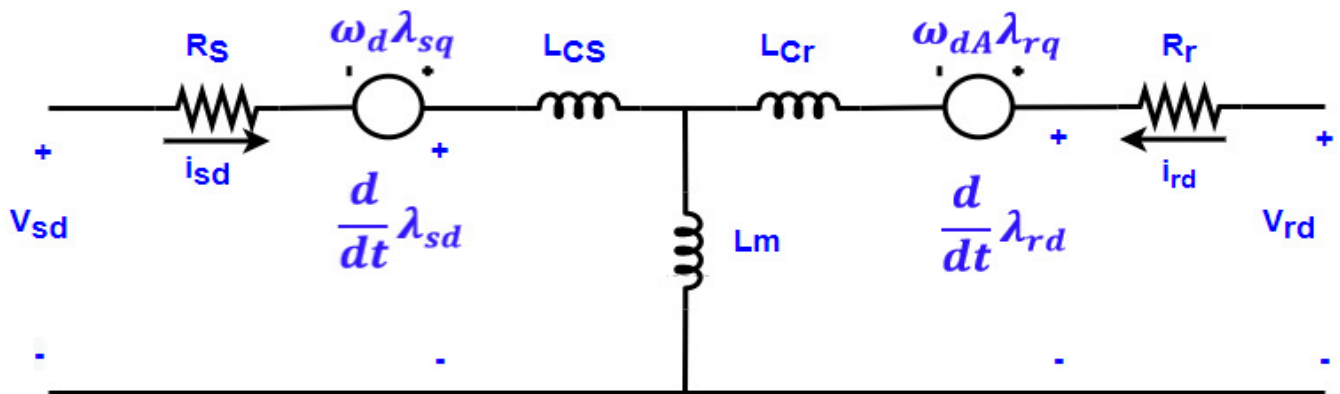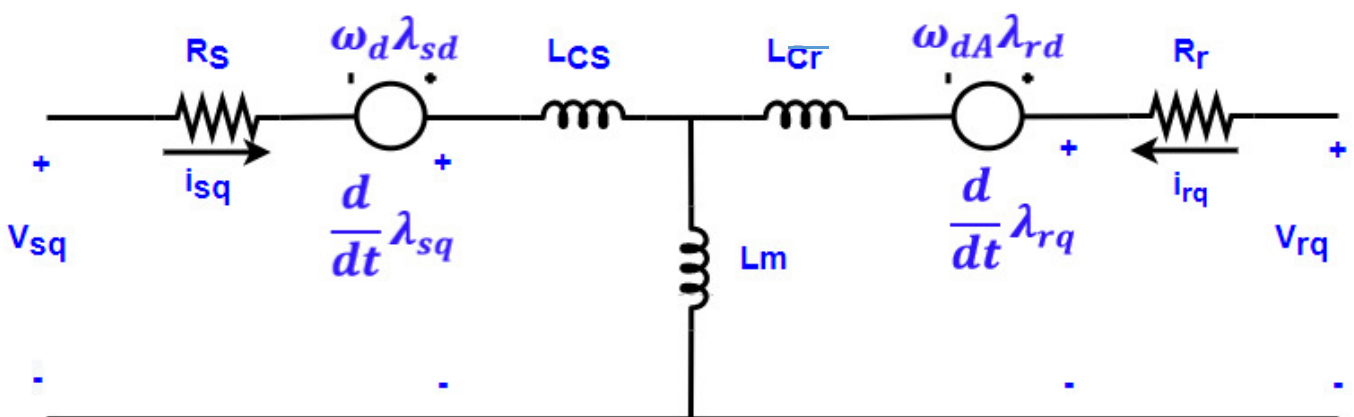**Figure 3.** Induction motor equivalent circuit for the d-axis.

Figure 4. Induction motor equivalent circuit for the q-axis.

The connection between $\alpha\beta$ and *abc* is given by

$$
\begin{bmatrix} V_\alpha \\ V_\beta \end{bmatrix} = \frac{2}{3} \begin{bmatrix} 1 & \frac{1}{2} & \frac{-1}{2} \\ 0 & \frac{\sqrt{3}}{2} & -\frac{\sqrt{3}}{2} \end{bmatrix} \begin{bmatrix} V_a \\ V_b \\ V_c \end{bmatrix}
\tag{13}
$$

Then, the voltage of *d* and *q* axis is

$$\begin{bmatrix} V_d \\ V_q \end{bmatrix} = \begin{bmatrix} \cos\theta & \sin\theta \\ -\sin\theta & \cos\theta \end{bmatrix} \begin{bmatrix} V_\alpha \\ V_\beta \end{bmatrix} \tag{14}$$

The three-phase stator and rotor currents' instantaneous values are finally deliberated by the succeeding modifications [41,42].

$$\begin{bmatrix} i_\alpha \\ i_\beta \end{bmatrix} = \begin{bmatrix} \cos\theta & -\sin\theta \\ \sin\theta & \cos\theta \end{bmatrix} \begin{bmatrix} i_d \\ i_q \end{bmatrix}$$
$$\begin{bmatrix} i_a \\ i_b \\ i_c \end{bmatrix} = \frac{2}{3} \begin{bmatrix} \frac{-1}{2} & \frac{-\sqrt{3}}{2} \\ \frac{-1}{2} & \frac{-\sqrt{3}}{2} \end{bmatrix} \begin{bmatrix} i_\alpha \\ i_\beta \end{bmatrix} \tag{15}$$

From the analysis of the D-q equivalent circuit, the differential equations are given by the following equations [43–45]

$$V_{sd} = R_s i_{sd} + \frac{d\lambda_{sd}}{dt} - \omega_d \lambda_{sq}$$
$$V_{sq} = R_s i_{sq} + \frac{d\lambda_{sq}}{dt} + \omega_d \lambda_{sd} \tag{16}$$

$$V_{rd} = R_r i_{rd} + \frac{d\lambda_{rd}}{dt} - \omega_{dA} \lambda_{rq}$$
$$V_{rq} = R_r i_{rq} + \frac{d\lambda_{rq}}{dt} + \omega_{dA} \lambda_{rd} \tag{17}$$

The flux linkages equation is given by

$$\lambda_{sd} = L_s i_{sd} + L_m i_{rd}$$
$$\lambda_{sq} = L_s i_{sq} + L_m i_{rq} \tag{18}$$

$$\lambda_{rd} = L_r i_{rd} + L_m i_{sd}$$
$$\lambda_{rq} = L_r i_{rq} + L_m i_{sq} \tag{19}$$

Equation (20) describes the self-inductance of three-phase induction motor

$$L_s = L_m + L_{ls}$$
$$L_r = L_m + L_{lr} \tag{20}$$

The currents can be written as

$$i_{sd} = \frac{\lambda_{sd} - L_m i_{rd}}{L_s}$$
$$i_{sq} = \frac{\lambda_{sq} - L_m i_{rq}}{L_s} \tag{21}$$

$$i_{rd} = \frac{\lambda_{rd} - L_m i_{sd}}{L_r}$$
$$i_{rq} = \frac{\lambda_{rq} - L_m i_{sq}}{L_r} \tag{22}$$

Substitute λ_{sd}, λ_{sq}, λ_{rd}, and λ_{rq}, in i_{sd}, i_{sq}, i_{rd}, and i_{rq}, and the currents can be demonstrated by flux linkages in Equations (23) and (24).

$$i_{sd} = \frac{L_r}{L_r L_s - L_m^2} \lambda_{sd} - \frac{L_m}{L_r L_s - L_m^2} \lambda_{rd}$$
$$i_{sq} = \frac{L_r}{L_r L_s - L_m^2} \lambda_{sq} - \frac{L_m}{L_r L_s - L_m^2} \lambda_{rq} \tag{23}$$

$$i_{rd} = \frac{L_s}{L_r L_s - L_m^2} \lambda_{rd} - \frac{L_m}{L_r L_s - L_m^2} \lambda_{sd}$$
$$i_{rq} = \frac{L_s}{L_r L_s - L_m^2} \lambda_{rq} - \frac{L_m}{L_r L_s - L_m^2} \lambda_{sq} \tag{24}$$

3. Simulation and Result Discussion of Three-Phase Induction Motor Dynamic Modeling

The value of parameters, namely, speed, d-q current, torque and three-phase voltage, is obtained from the d-q representation of AC motor, which is constructed using Simulink. The basic need of this dynamic model in state space form is that it is essential in performing the transient analysis of the induction motor or particularly for simulation study in the computer by using MATLAB/SIMULINK. The squirrel cage type of induction motor requires three inputs: the rotor speed, three-phase voltage and fundamental frequencies. When we feed these three inputs, the outputs are the rotor speed, three-phase currents and torque [46–48]. The basic prerequisite of the d-q model is the transformation of the entire three-phase variable to the two-phase rotating frame. As a result, the AC machine design will be constituted by blocks that transform the three-phase voltage to the d-q frame and currents back to three phases. In addition, a vector of field-oriented control, which is considered considerable presentation drive control, is established on the dynamic d-q design of the induction motor. The motor can be modeled in a rotating and stationary frame. The main variables considered are the machine state space equation in the rotor frame with flux linkages illustrated in Figure 5. The simulated model is easy to develop since Simulink is a model operation programmer [49–52].

(**a**)

Figure 5. *Cont.*

(**b**)
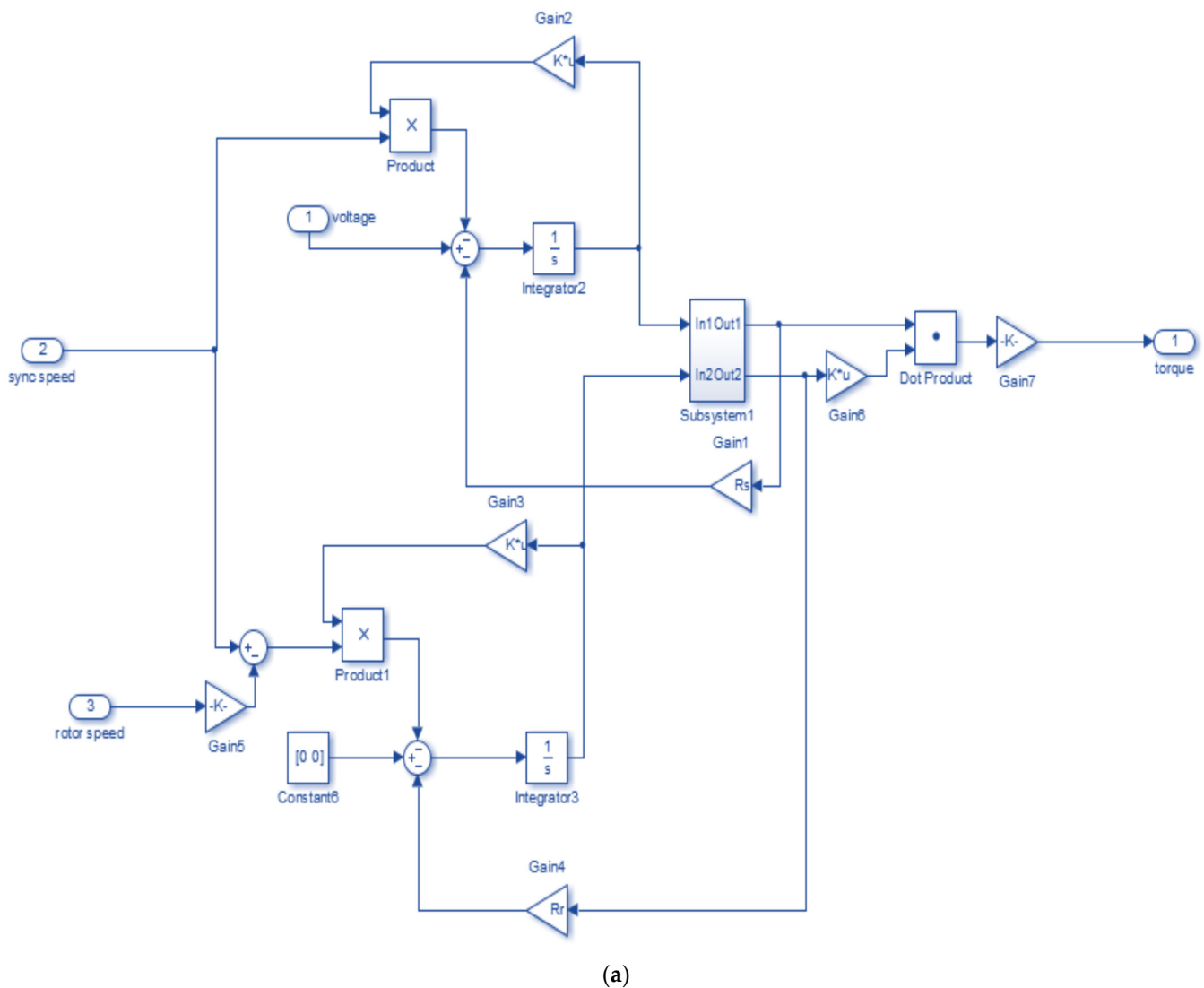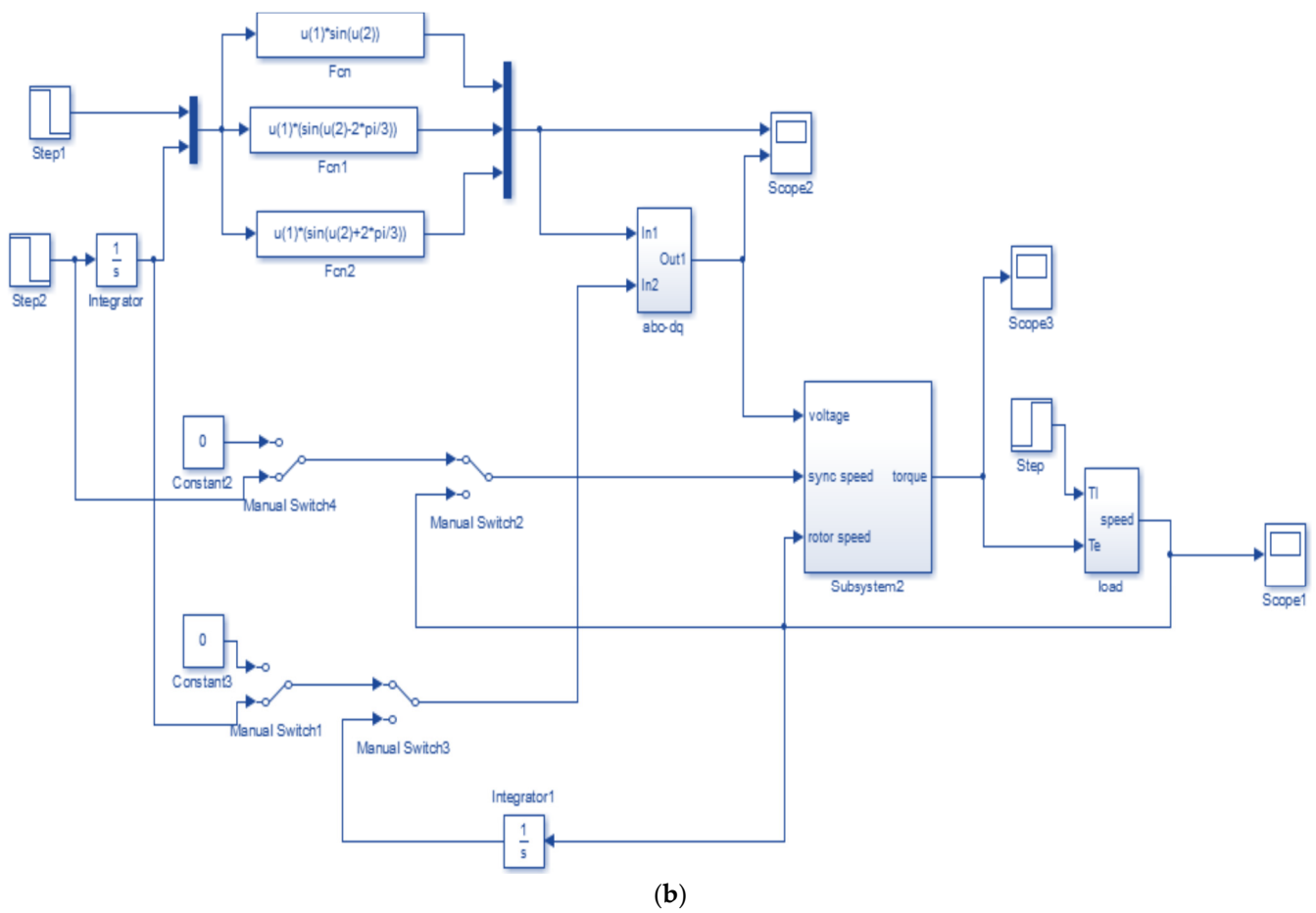
Figure 5. (**a**) Subsystem of dynamic modeling of three-phase induction machine. (**b**) Simulation of dynamic modeling of three-phase induction machine.

The induction motor parameters, namely, torque, speed, rotor and stator current, are established from the simulation of dynamic models as depicted in Figure 5. The simulation for flux, abc to dq and load are illustrated in Figures 6–8, respectively.
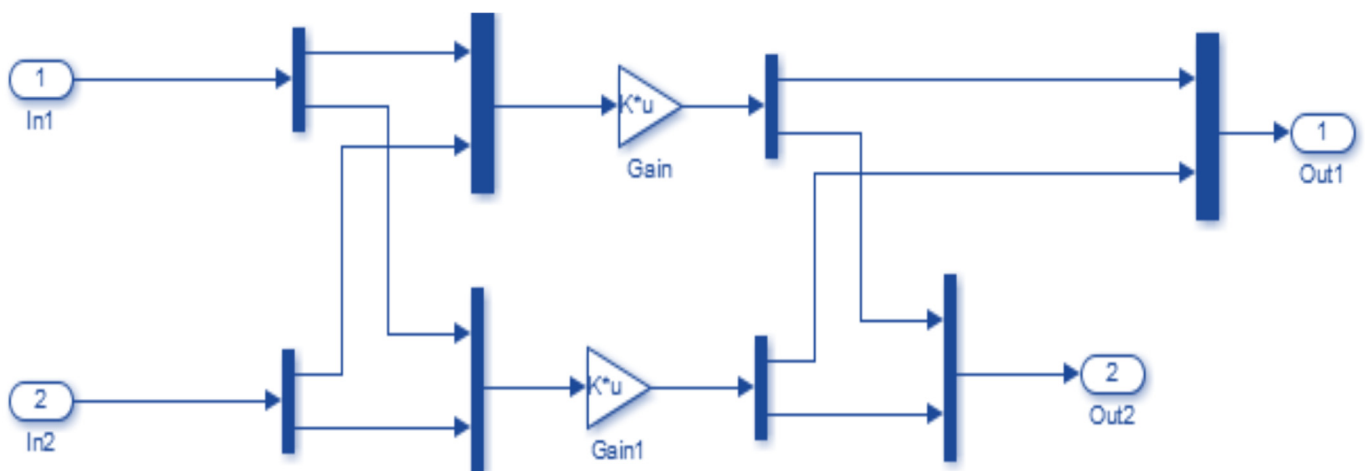

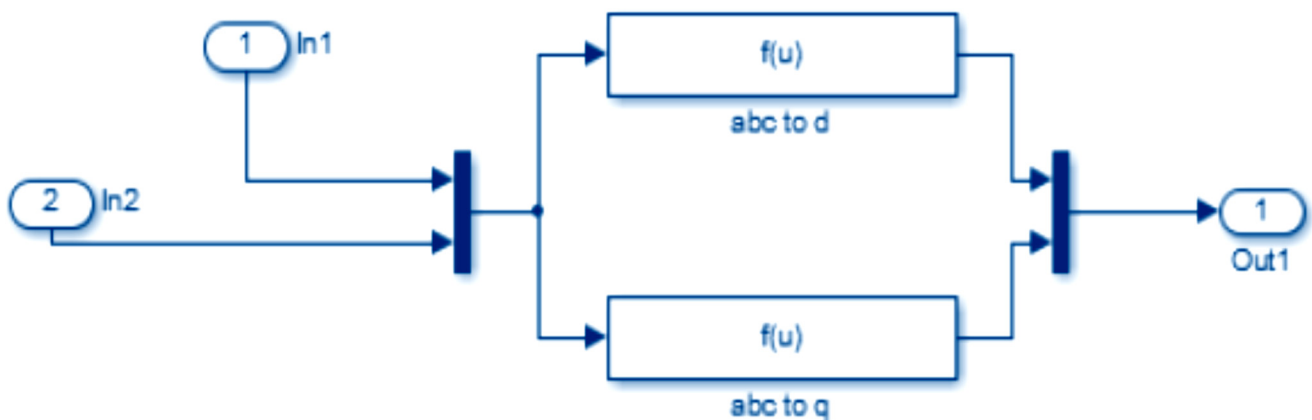
Figure 6. Flux current relation.
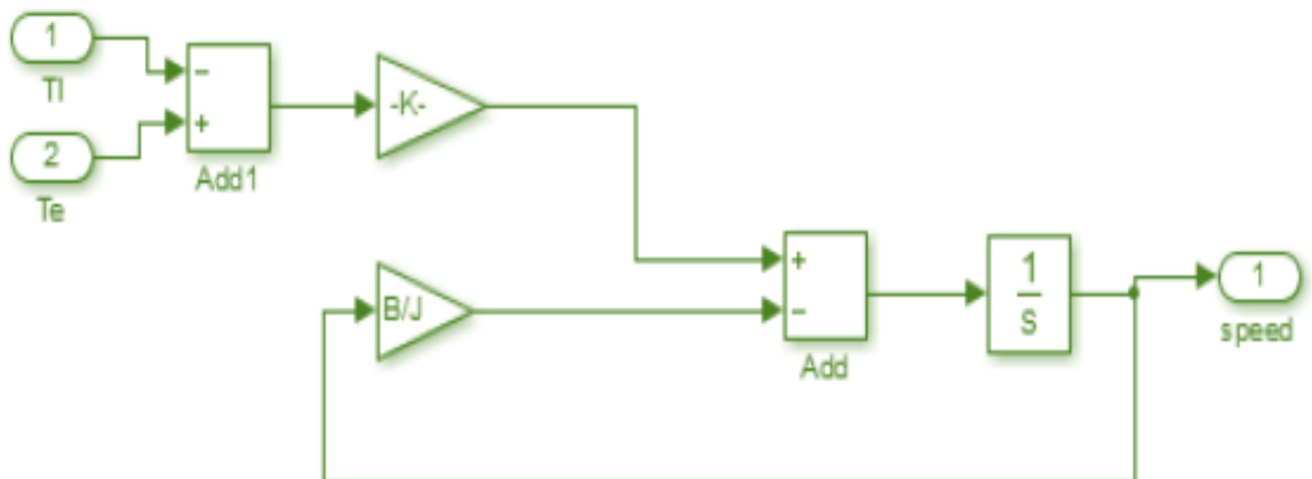
Figure 7. ABC to dq transformation.

Figure 8. Load for dynamic modeling.

The induction motor simulation results are given with the succeeding specifications: R_s = 6.03 ohms, R_r = 6.085 ohms, L_m = 0.4893 H, f_b = 50 Hz, p = 4, J = 0.011787, B = 0.0027, L_r = 0.5192 H, L_s = 0.5192 H, L_{rl} = $L_r - L_m$, L_{sl} = $L_s - L_m$, T_s = 2×10^{-6} N-M, T_r = L_r/R_r. The output voltage of three-phase induction motor is depicted in Figure 9 with the amplitude 340 Volts and stator current in Figure 10.

Figure 11 represents the motor speed and torque realization for different time instances for an induction motor. At an instant of precisely 1.5 s, speed is noted to be 1490 rpm. After this instant per time, it remains constant at 1490 rpm. Consequently, the torque oscillates from the values of 2 to 85 N-M to the speed of 1490 rpm. After this, the torque remains at 0. Therefore, this figure helps in concluding that the induction motor can reach the speed of 1490 rpm with a stable condition. A d-q model of an induction motor developed with the use of Simulink has been presented here. This model has varied applications and is beneficial for using electric machines, and power electronic courses can be employed in laboratories as a research tool. A block model method was studied for the motor model construction. This allows the students to resolve the issues related to the reference frame theory. The enhanced model is intuitive, simple to use and gives the case to access all motor parameters for monitoring and comparison purposes. Besides this, this model can help study the induction motor's dynamic behavior. New subsystems can be added to the presented model to implement various control schemes. In addition, the presented model can be clubbed with different inverter topologies and pulse width modulation (PWM) techniques after making a few minor modifications to the model.
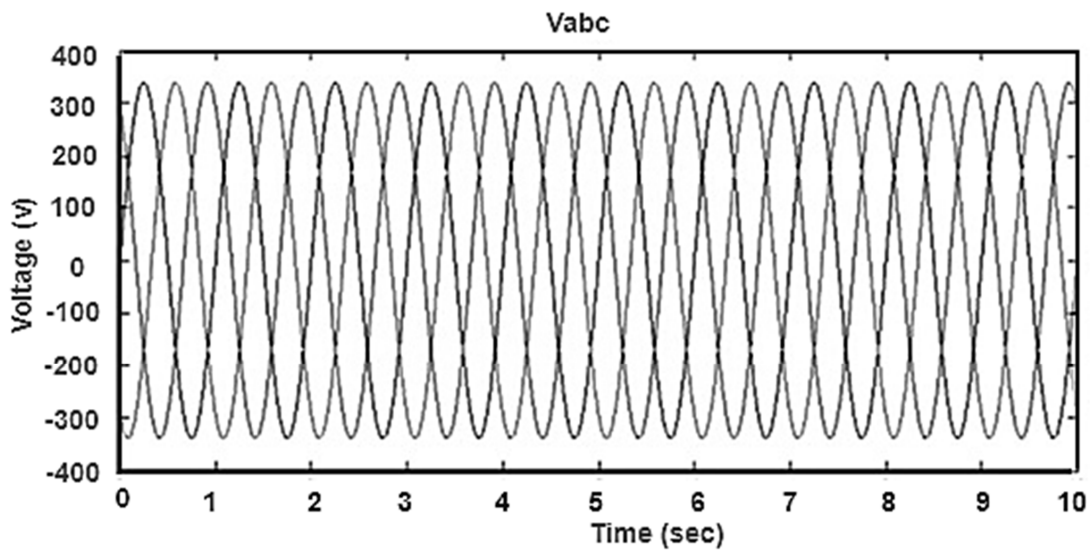
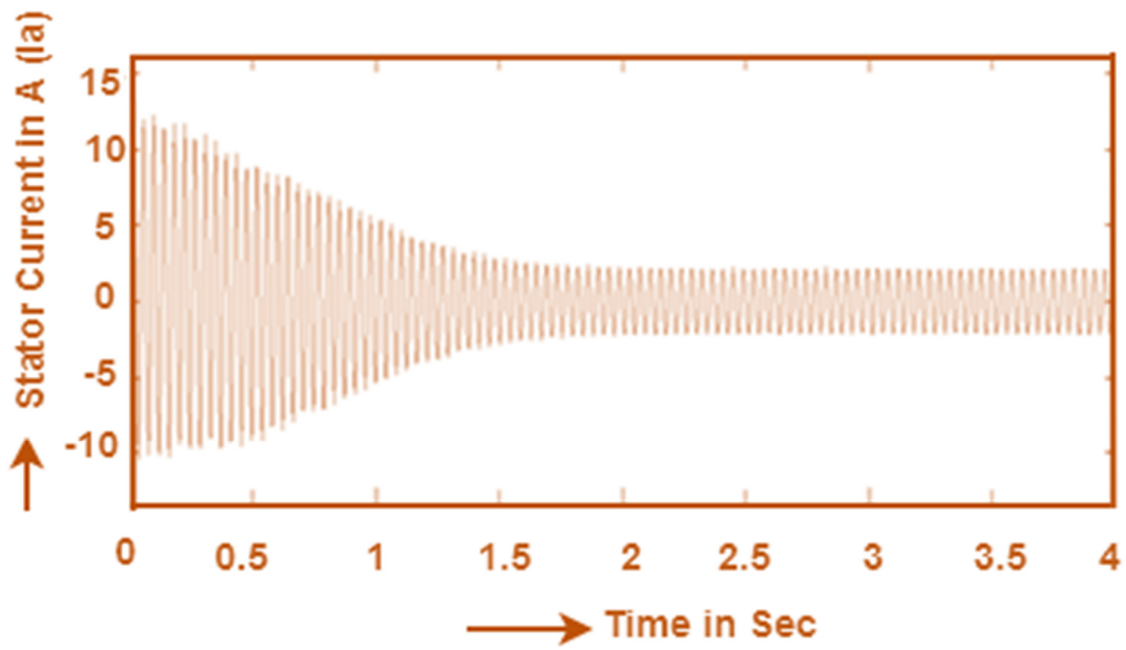**Figure 9.** Output voltage of three-phase induction motor.

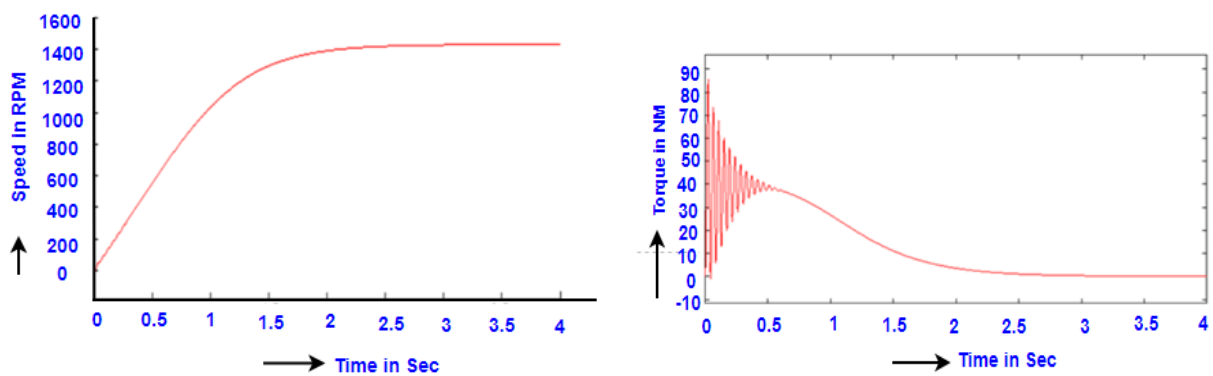**Figure 10.** Stator current.

Figure 11. Speed and torque response of an induction motor.

4. Parameter Estimation of Three-Phase Induction Motor

An Ac motor is commonly employed as a machine for application in high-interpretation drives. Detailed knowledge of parameters subjected to an induction motor is required to control such drives. If, by chance, the value of the parameter used in the controller mismatches, the overall drive performance will degrade. The parameters of an induction motor are the stator's resistance, the rotor's inductance of stator and rotor, magnetizing reactance, the number of poles, frictional coefficient, speed, torque, etc. The electrical parameters of the induction motor are approximated by a DC resistance test, no load test, and blocked rotor test with equivalent circuit calculations. The number of poles, friction coefficient and moment of inertia is taken from old literature with mathematical formulae. To avoid the mismatch of motor parameters with controller parameters, estimating parameters play a vital role in an induction motor. Parameters have been approximated by online and offline methods for use in high-performance drives, the asynchronous motor. The frequently used method to control AC machines is the field control method. It is used in high implementations of induction motors or applications of electric drives. A perfect value of some of the motor quantities is required by rotor flux-oriented RFO so that it can achieve robust control in the induction motor. To figure out what parameters are required for control, an RFO control scheme is used. If the variable and the actual values fail to match, the detuned operation occurs oriented (RFO) control needs a perfect value of at least some of the motor parameters. In the past, an extensive study has been carried out on the influence of parameter changes on different vector control algorithms, and detailed discussion concluded based on this study is obtainable in several books. An induction motor vector control can be employed within a drive of torque and speed. The torque drive exhibits the largest sensitivity to the increased parameter value of the mentioned drives. The speed control applications are affected by the changes in rotor parameters [53–56]. These effects can be eliminated with the help of a PI controller. A PI controller helps by reducing the negative consequence of the parameter detuning to a considerable level. This way, if there happens to be a mismatch between the actual motor values, the flux position and the position assumed by the controller can be quickly figured out. Factors such as temperature, frequency and saturation affect the induction motor parameters and bring a change in their values. The actual motor flux is constituted by x and y axis composing, which is guided to a loss of dissociates flux and torque control. This leads to a decrease in the performance of the drive. The solution to avoid such saturation is a motor controller with an accurate induction motor parameter value obtained during the driver's initialization from measurements. Several tests have been carried out lately to figure out the required parameter values of a motor-supervised induction fed by a motor driver inverter. Such parameters were given the name "Offline parameter identification methods". Numerous possibilities also exist these days, which help estimate the parameter values during time operation. During driver operation, the methods that qualify parameter transformation are known as "Online parameter estimation methods". This paper gives a review of the methods employed for identifying and calculating offline and online parameters of an induction motor. The offline or online tracked parameters can be distinguished with the help of vector control schemes.

The rated value of magnetizing inductance, the resistance of rotor and stator, and the leakage inductance of stator and rotor on transient stator inductance are the parameters required in case the drive employs a constant rated flux reference magnetizing curve will be required in cases where the drives function with a changeable reference of flux. The induction motor is utilized most frequently in electric traction applications because of its better performance and lower initial and maintenance cost. Installing speed sensors to the drive motor results in several drawbacks, including decreased reliability, increased pricing, and footprint. Therefore, this paper review has been focused on sensorless induction motor drives. An induction motor's rotor speed is found using the studied stator voltage and current as the sensorless drive. Several methodologies can be utilized to provide peed estimation for sensorless drives. These strategies were developed considering several

factors, including sensitivity and accuracy, which are adversely affected by parameter variations [57–59].

4.1. Significance of Parameters

For transient purposes, it is crucial to have a precise model of a drive motor so that a detailed analysis can be conducted. Inducing such motor injury in the real world for drive motors is hazardous. Investigating these processes with mathematical modeling selects the appropriate protection and control devices essential for reliable operation. To accurately simulate the motor, it is vital to know the equivalent circuit parameters. Motor settings intended for the scientific record may vary up to 20% from one manufacturer to another due to technical or observational errors. Therefore, engineers demand precise motor values to craft robust drives. Moreover, suppliers must devise a strategy to address this challenge, as only commercial indices provided alongside technical documents are valued [60].

Stator resistance: The current obtained from the magnetic field of the stator winding is used to produce torque in the induction motor. The rotor resistance R2 has a vital role in the working of an induction motor. Apart from this, R1 resistance decides the torque–speed curve, which determines the speed at which the pull-out torque occurs. To determine the resistance, a blocked rotor test can be performed. This test determines the resistance of the total motor circuit. However, this test finds only the total resistance. It is mandatory to know the value of R1 so that it can be subtracted from the total to find R2. The DC resistance is a test for determining R1 independent of parameters such as R2, X1 and X2. To carry out this test, the induction motor stator winding is primarily supplied with the DC. The main objective behind supplying DC is that there is no voltage being influenced inside the rotor circuit as an output of which rotor current and the reactance of the motor becomes zero. Therefore, stator resistance is the only quantity in the motor that limits the current. Hence, in this way, the rotor resistance can be determined. This parameter's availability is only present when the "equivalent circuit of parameter for the parameterization" is selected [61].

Rotor Resistance: The rotor resistance circuit considerably affects the occurrence of maximum torque speed. This can be found in the torque–speed curve. Rotor resistance and starting torque are directly proportional to each other, which mean a high starting torque will be obtained by a high rotor resistance, which will lead to rapid acceleration of the mechanical system. This acceleration is required since starting the stator current significantly exceeds the rated current. A relatively high slip occurs during normal conditions due to high rotor resistances. Torque corresponds to rotor joule losses allocated by slip and significant resistance. The increase in losses is due to high resistance, which decreases the efficiency during regular operation. These points lead to a problem as for the most significant applications; it is advisable to have (1) very high starting torque and (2) improved efficiency at a constant speed. However, two facts are conflicting. The first one says that the prototype with ample starting torque will have less efficiency at the rated speed, while the other states that the design with high frequency will have low starting torque. To solve these two conflicting requirements, the steps that must be taken are (1) careful consideration of the application requirement and (2) design of a motor with variable rotor resistance. The value of the stator and rotor RMS current magnitude of the motor increases drastically, and this effect keeps decreasing with modulation frequency and as the voltage varies (increases). Losses will also increase due to the increase in RMS current, as a consequence of which the motor winding temperature will rise. Subsequently, the ageing process gets accelerated [61].

Stator Inductance: The leakage reactance is basically defined as the impedance/resistance offered by the leakage inductor. Similarly, the inductance offered by the stator winding is called the stator inductance. Its default value is considered to be 0.02 H. This parameter is observable when "by equivalent circuit parameters for the model parameterization parameter" is selected [61].

Magnetizing Inductance: Magnetizing Inductance can be the self-inductance of an inductor with a magnetic core. The parameter-magnetizing inductance of the stator is

visible only when "equivalent circuit parameters" for parameterization of parameters are selected. Its effect is usually the smallest, and it is not easy to estimate the value from motor parameters. Its typical value is 25 times the inductance of the stator value. The standard value is 0.5 H [62].

Rated mechanical power: Electrical circuits are rated in electrical input power. Generally, a device's power value is the largest power input authorized to flow across notable equipment. It can involve the maximum and average power depending on the application. Here, mechanical is the power motor provided while running at rated speed. The standard value is taken as 825 W. This parameter is visible only when "by equivalent circuit parameters for the model parameterization parameter" is selected [62].

Rotor impedance: asynchronous motor with slip ring is benefited where conditions such as high load demands and variable speed are to be met or where the motor needs to be initiated under a large load. The main advantage of using slip-ring induction motors is that it provides a wide range of liberation for the engineers' starting and control speed values. Applications of these motors include crane and hoist control. To achieve smooth start and speed control, register controllers are used in the rotor circuit. Several recent investigations have shown that a desired torque speed characteristic can be obtained by inserting a simple passive frequency-sensitive network. By carefully selecting the network parameters, starting currents can be reduced, and improved torque-to-current ratio can be achieved. Hence, it is mandatory to understand the results of rotor impedance on presentations of induction motors, which will further help in understanding the industrial system preferring to incorporate slip ring induction motors generally [62,63]. Factors that agitate the parameters of induction motor are listed in Table 1.

Table 1. Factors that agitate the parameters of induction motor.

Factors	Affecting Mechanism	Parameters Affected
Temperature reorder	Change in temperature changes the degree of ageing and also wear and tear of motor	Stator and rotor resistance
Frequency reorder	Due to frequency changes of current skin effect comes into action, which in turn affects the rotor's slot	Resistance and inductance of rotor
Magnetic saturation	When the magnetic is soaked, the resistance of the rotor is enlarged, and the inductance reduced	Rotor resistance and inductance, the coefficient of leakage inductance
stray loss	Higher-order harmonics are produced because of eddy current and hysteresis loss which are produced by magnetic flux leakage	the inductance of the stator and rotor, mutual inductance

4.2. Methods of Parameter Estimation and Its Test

Measurement of stator winding resistance—the test of each stator winding is measured individually, and the condenser is omitted when the capacitor starts the motor. To perform a blocked rotor test, primary and stator winding are dealt with separately. For each case, input voltages, amperes and watts are measured. This measurement is conducted (up to 40% of rated voltage) to avoid any extra short circuit current and heating. To perform the no load test, a rated voltage is selected. The primary winding is excited, and the input voltage, current and power are measured. For carrying out the windage and friction loss test, the voltage in the motor is gradually decreased until the point where the motor will only run. The power input is measured. This gives the friction and windage losses [64]. The two primary techniques for parameter estimation are Offline and Online techniques.

4.2.1. Offline Techniques for Identifying Parameters of Induction Motor

In common practice, one manufacturer contributes to an inverter with field-oriented control (FOC), while the machines come from further processors. Under such a situation, the controller's data cannot be set in foster. The onsite setting of the parameters has to be conducted after the inverter has been connected to the machine. This guided the procedure

of self-commissioning for vector-controlled induction machines. This concept authentically makes the controller determine all the parameters needed for FOC in an AC motor. The electrical procedure of checking and determinations is carried out by first switching on the controller. There is a possibility that the induction machine would be coupled to a load already. The main aim of self-commissioning is to trace the data at a halt while the induction machine is combined with the load.

Tracing such parameters is carried out with a one-phase supply to the machine. The types of excitations can be used AC or DC [65]. DC excitation, however, is considered ideal in the case of self-commissioning. To find the value of the stator resistance, appeal DC voltage and resistant DC constant state current are used. The rest of the parameters are based most regularly on transient current reactions that successfully apply the DC voltage self-commissioning schemes described in conventional methods in this approach. The methods that required the same states to be pleased during commissioning may be regarded as suitable for commission but appropriate for self-commissioning. Some of these methods are the ones in which the rotation of the machine is allowed. This is because of the need for substantially high difficult mathematical action of the results during measurements compared to the self-commissioning procedure. For example, the algorithm stated in previous methods depends on some test in the one-phase power to the machine. At the same time, the old methods require the application of pseudo-random sequence voltage stimulation and an adaptive observer [66–68]. Parameters that are determined match with sinusoidal supply on the condition that the calculations are dependent on the basic components. This feature is explored in conventional methods, where the parameters are identified by using the DC, no load and pseudo-locked rotor tests [69,70].

DC Resistance Test

Stator resistance is the simplest element to be determined. To determine the value of resistance, the text is conducted on an isolated motor to check the resistance of stator windings. A low-reading ohmmeter or a high-resolution digital multimeter is used to achieve an accurate measurement. The values that are obtained from the DC test are approximate values. Skin effects and temperatures that are produced due to AC supply are not taken into consideration. However, this approximation is quite reasonable. Initially, the motor is isolated. This can be conducted mechanically or electrically [64,65]. Next is the identification by using the millimeter. The DC resistance test of a tree-phase induction motor simulation circuit is shown in Figure 12.

No Load Test

The no-load test provides data about the rotational losses and exciting current and is somewhat the same as the open circuit test on a transformer. To carry out the test, an equitable rated voltage is applied on the winding of the stator at a rated frequency. The slip of the machine is nearly zero, which makes the machine rotate at almost a synchronous speed. In this study, there is no load on the machine. The slip is minuscule. This involves the current, and resistance in rotor winding can be neglected compared to the magnetizing current. A magnetizing branch is present in the equivalent circuit of an induction motor at no load conditions. The value of the above-stated parameter can be determined by evaluating the current, power, and voltage at no load. No load test is studied by managing the motor at an estimated line-to-line voltage. The values so obtained are noted down. These are no-load current values and total three-phase active power [64,65]. The mathematical equation that was derived from the equivalent circuit helps to identify the electrical parameter of the induction motor.
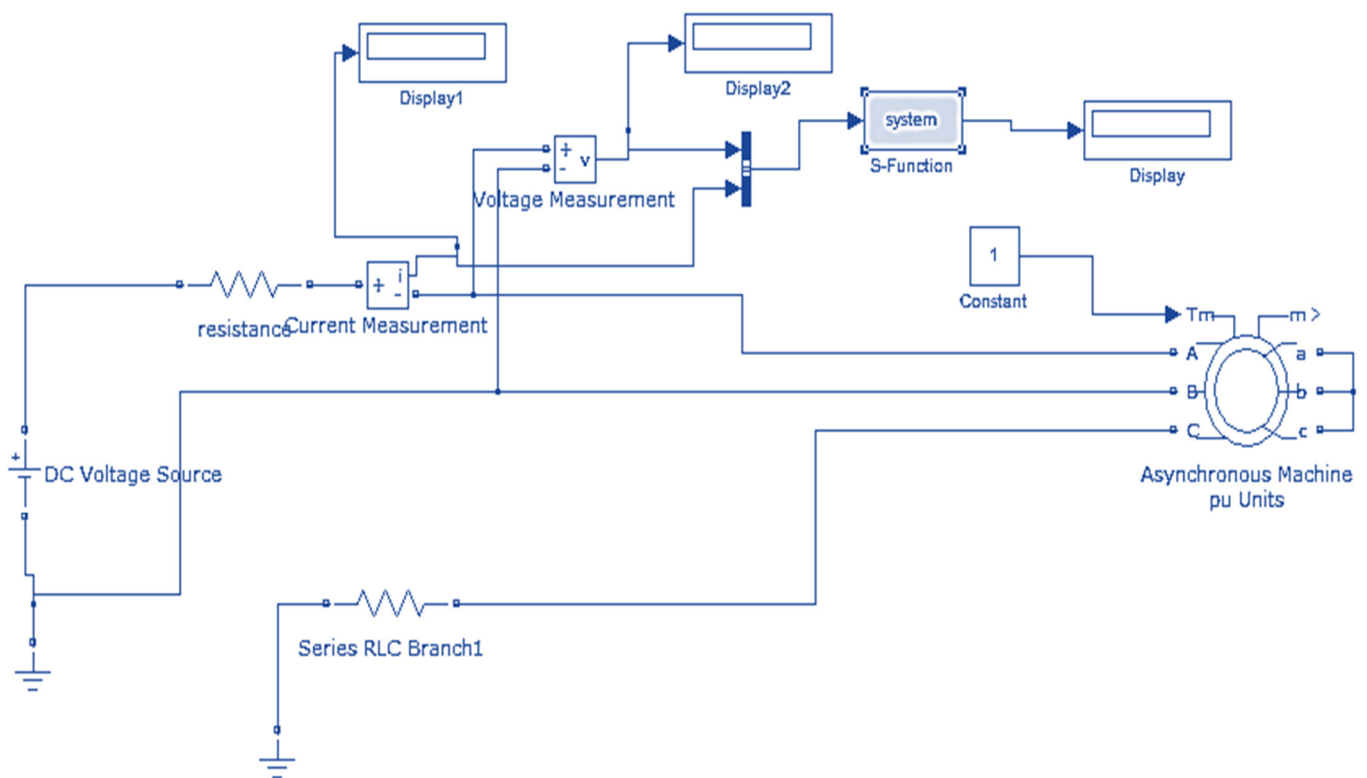
Figure 12. DC resistances test.

Blocked Rotor Test

The locked rotor test provides data about leakage impedance and resistance of rotors. To circulate the rated current, a low voltage is supplied to the windings of the stator while the rotor remains at a standstill state. The voltage and power to the phase are measured. The following equivalent circuit is obtained due to no rotation slip, where s = 1. As the name suggests, in the blocked rotor test, the rotor is blocked from rotating. As we know, the rotor is not allowed to rotate, and the mechanical speed is zero. For the blocked rotor test, the value of the slip is taken as unity. Therefore, the rotor current essentially exceeds the current value in the circuit's excitation limbs, concluding that the branch mentioned above can be omitted.

A mathematical equation derived from the equivalent circuit is used to calculate the electrical parameters of the induction motor. The extensive analysis of drives of induction motors, including the decoupling control and without sensor control, depends on the accuracy of the parameters of the machine. They make use of equivalent machine models for this purpose. To date, the blocked rotor test and the no-load test are traditional methods for measuring motor variables. However, these methods have some disadvantages. They require additional means for locking or rotating the rotor at synchronous speed. Another drawback is that the testing conditions differ from the actual operating conditions. During the regular induction motor operation, the slip frequency is identified as less than the rated slip. The slip frequency of induction motors during a locked rotor test is equal to the power source frequency. Therefore, an inaccuracy in measurements occurs because of high slip frequency. To eliminate such inaccuracies, the auto commissioning function includes auto measurement of motor parameters. Auto commissioning is a significant request for modern adjustable drive systems in the market [65–70]. Survey for parameter estimation—offline identification methods is given in Table 2.

Table 2. Survey for parameter estimation—offline identitation methods.

Recognition Method	Recognition Principle	Recognition Parameters	Benefits	Limitations
Blocked rotor test	The rotor is blocked from rotating by applying a full load. Then different values are noted down at the rated current.	Resistance and inductance of stator, mutual inductance.	The identification parameters mentioned are calculated easily.	Proper control of load is needed, and skin effect appears.
No Load test	The rotor runs at synchronous speed without any load.	Excitation resistance and reactance.	Convenient.	Applying no load is inconvenient.
Auto tuning method	We tune the accurate inverse of the time constant of the rotor in this method.	Stator and rotor resistance.	Precise and reliable.	This method is favourable when used with a frequency converter in a control system.
Least square method	Data is sampled and measured and a curve is drawn with least square values and results are obtained.	Rotor resistance and inductance.	Highly accurate and precise.	A large amount of data analysis is required with lot of tedious time calculations.

Parameter Mismatch with Measured Data

Manufacturers provide a data sheet listing the electrical data for the AC motor equivalent model. This listing is based on calculated test data, such as manipulating the quality tests in IEEE std112, for instance. However, when it comes to computing the motor speed–torque curve employing these data, it is found that the data sheet values and the values obtained after computing differed significantly. The torque–speed graph entails the equivalent circuit, and the manufacturer's sheet showed variations. The reason behind this variation is that the equivalent circuit model is just a simplified version of reality. An equivalent model with sustained parameters is preferred for representation because it is reasonably accurate for the full range of sip values. The parameters of the equivalent circuit are not sustained and differ with slip frequency. The measured electrical data for various slips provided by the manufacturer will undoubtedly differ from those provided by some other manufacturers. Due to the teeth' core saturation and temperature, the parameters of AC motor will vary. By the DC resistance test, the resistance of the stator is generally measured, but the AC resistance will vary due to its temperature effect. The leakage reactance at locked rotor conditions gets reduced because of the soaking of the leakage trail of the stator and rotor magnetic field during direct on line (DOL). However, to simulate total load currents, a leaked rotor test is carried out at reduced voltages [70].

4.2.2. Online Assessment Techniques for Speed Estimation of Sensorless Drive

The development of motor time constant online estimation methods is where major effort has been put into. These are further categorized and classified into four subgroups because of the multiple prepared solutions of adverse nature [71–73]. The structures of the fundamental basic speed methods are shown in Figure 13. In short, it can be summarized that the speed estimation technique is classified as slip calculation and direct synthesis from state equations.
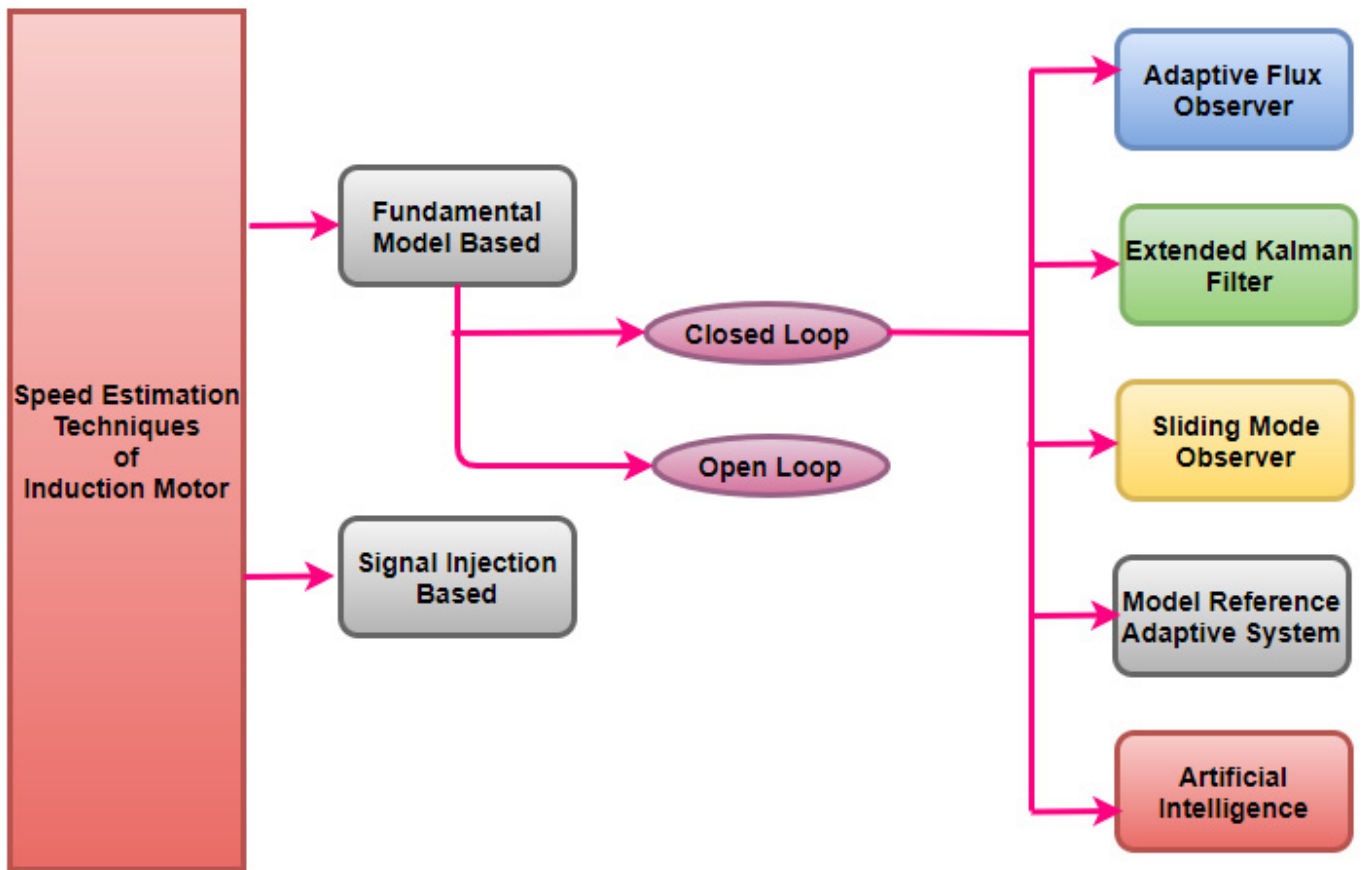
Figure 13. Speed estimation methods.

Open Loop Observer

From the stationary reference frame, the rotor fluxes of the induction motor are described as follows [58–60]:

$$
\begin{aligned}
\frac{d}{dt}\psi_{dr} &= \frac{L_r}{L_m}V_{ds} - \frac{L_r}{L_m}\left(R_s i_{sd} + \sigma L_s \frac{d}{dt} i_{sd}\right) \\
\frac{d}{dt}\psi_{qr} &= \frac{L_r}{L_m}V_{qs} - \frac{L_r}{L_m}\left(R_s i_{sq} + \sigma L_s \frac{d}{dt} i_{sq}\right)
\end{aligned}
\tag{25}
$$

$$
\begin{aligned}
\frac{d}{dt}\psi_{dr} &= \frac{L_r}{L_m}\left(V_{ds} - R_s i_{sd} - \sigma L_s \frac{d}{dt} i_{sd}\right) \\
\frac{d}{dt}\psi_{qr} &= \frac{L_r}{L_m}\left(V_{qs} - R_s i_{sq} - \sigma L_s \frac{d}{dt} i_{sq}\right)
\end{aligned}
\tag{26}
$$

$$
\frac{d}{dt}\begin{bmatrix} i_{s\alpha} \\ i_{s\beta} \\ \psi_{s\alpha} \\ \psi_{s\beta} \end{bmatrix} = \begin{bmatrix} -a_1 & 0 & a_2 & a_3\omega_r \\ 0 & -a_1 & -a_3\omega_r & a_2 \\ a_4 & 0 & -a_5 & -\omega_r \\ 0 & a_4 & \omega_r & -a_5 \end{bmatrix} \begin{bmatrix} i_{s\alpha} \\ i_{s\beta} \\ \psi_{s\alpha} \\ \psi_{s\beta} \end{bmatrix} + \frac{1}{\sigma L_s}\begin{bmatrix} V_{s\alpha} \\ V_{s\beta} \end{bmatrix}
\tag{27}
$$

$$
\begin{bmatrix} i_{s\alpha} \\ i_{s\beta} \end{bmatrix} = \begin{bmatrix} 1 & 0 & 0 & 0 \\ 0 & 1 & 0 & 0 \end{bmatrix} \begin{bmatrix} i_{s\alpha} \\ i_{s\beta} \\ \psi_{s\alpha} \\ \psi_{s\beta} \end{bmatrix}
\tag{28}
$$

Substitute the above equation into the following component form:

$$
\frac{dx}{dt} = Ax + Bu \;\; \& \;\; Y = Cx
\tag{29}
$$

Equation (30) describe the state equation for the parameter estimation of the induction motor. Where

u—input of the system;

y—output of the system;

x—state vector;

A, B, C are constant matrices.

$$\frac{dx}{dt} = Ax + Bu + G(Cx - Y) \tag{30}$$

where

$$A = \begin{bmatrix} -a_1 & 0 & a_2 & a_3\omega_r \\ 0 & -a_1 & -a_3\omega_r & a_2 \\ a_4 & 0 & -a_5 & -\omega_r \\ 0 & a_4 & \omega_r & -a_5 \end{bmatrix} \tag{31}$$

where

$a_1 = \frac{1}{\sigma L_s}\left[R_s + R_r \frac{L^2_m}{L^2_r}\right]$, $a_2 = \frac{1}{\sigma L_s}\left[\frac{R_r L_m}{L^2_r}\right]$, $a_3 = \frac{1}{\sigma L_s}\left[\frac{L_m}{L_r}\right]$, $a_4 = \left[\frac{R_r}{L_r}\right]$, $a_5 = \left[\frac{R_r L_m}{L_r}\right]$.

$$p\,\psi_{dr} = \frac{L_m}{T_r}i_{ds} - \omega_r\psi_{qr} - \frac{1}{T_r}\psi_{dr} \;\&\; p\,\psi_{qr} = \frac{L_m}{T_r}i_{qs} - \omega_r\psi_{dr} - \frac{1}{T_r}\psi_{qr} \tag{32}$$

The angle of the rotor flux vector given by

$$\theta_e = \omega_e t = \tan^{-1}\left(\frac{\psi_{qr}}{\psi_{dr}}\right) \tag{33}$$

where

$\psi_{qr} = |\psi_r|\sin\omega_e t$, $\psi_{dr} = |\psi_r|\cos\omega_e t$.

$$\theta^*e = \omega_e = \frac{\psi_{dr}\psi_{qr}{}^* - \psi_{qr}\psi_{dr}{}^*}{\psi_{qr}{}^2 + \psi_{dr}{}^2} \tag{34}$$

Substituting Equations (31) and (32) in (34), the estimated speed is given by

$$\omega_r{}^* = \frac{1}{\psi_{r2}{}^*}\left[(\psi_{dr}\psi_{qr}{}^* - \psi_{qr}\psi_{dr}{}^*) - \frac{L_m}{T_r}(\psi_{dr}i_{qs}{}^* - \psi_{qr}i_{ds}{}^*)\right] \tag{35}$$

The assignment of the several gains, G and PI gains, determine the precision of speed calculations. Based on the pole placement approach, a representation of the observer gain G is performed. Stability at all speeds can be achieved by keeping the observer poles proportional to the motor poles. So, the parameter variation still tends to affect the accuracy of this method. This effect is more predominant in the case of low speeds as observer gain G is dependent upon induction motor parameters. The diagrammatic representation of the open loop observer is displayed in Figure 14, which is straight forward and has less computational time.

Adaptive Flux Observer

For AC motor drives, the indirect decoupling control method is employed. This method requires a speed sensor such as a shaft encoder, so that both speed and torque control can be achieved; however, this method is not very pragmatic since the direct decoupling control method with flux estimation, which was a pure integrator, does not need the speed sensor to control the torque. Moreover, another reason for its practicality is that the flux estimator does not perform well at low speeds. The flux valuation pole lying on the plane is conscious of the voltage sensor offset and variation in the resistance of the stator. Therefore, several field-oriental methods that do not require the use of speed sensors have been proposed. Out of all the proposed methods, some of these methods are

applicable. Apart from this, some methods are unstable in low-speed regions, as a pure integrator is used for the flux calculations, as mentioned above. Therefore, based on the adaptive control theory, a new technique of evaluating AC motor speed, a speed adaptive flux observer, has been suggested. To allocate poles arbitrarily, the observer has been used. It can also be adapted to the direct decoupling control in the low-speed region [74–76].
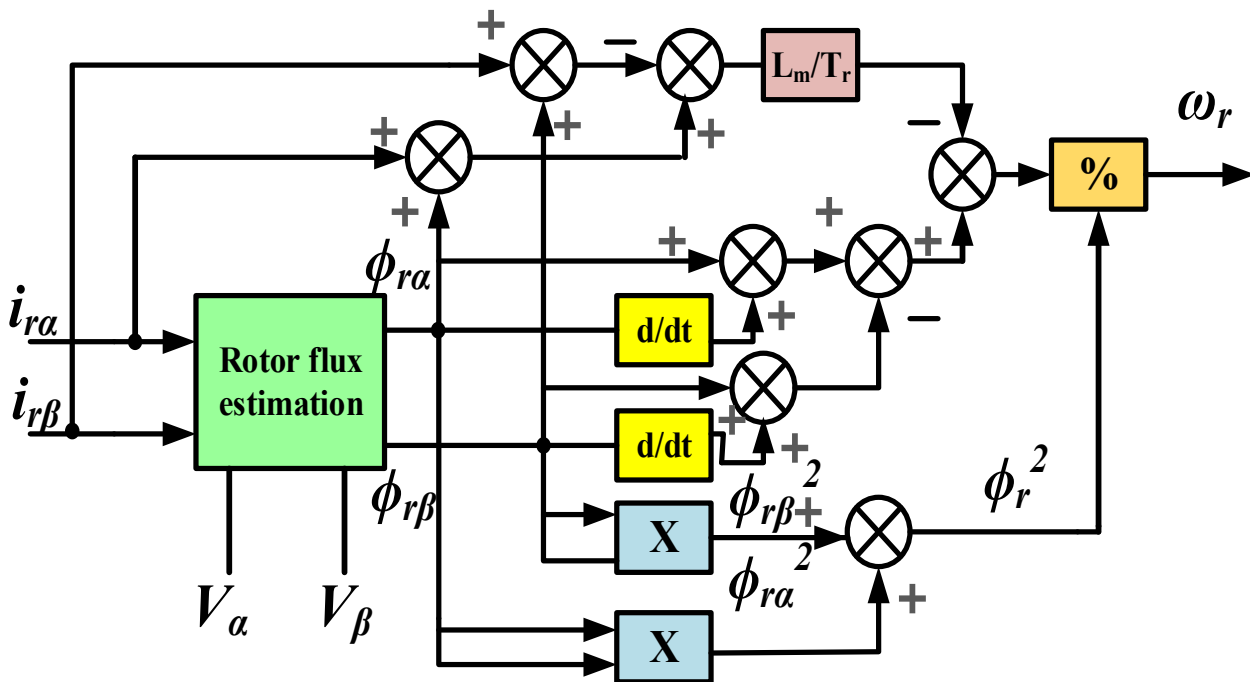
Figure 14. Open loop observer.

The state equation in the stationary reference frame is described by

$$\frac{d}{dt}\begin{bmatrix} i_s \\ \varphi_r \end{bmatrix} = \begin{bmatrix} A_{11} & A_{12} \\ A_{21} & A_{22} \end{bmatrix}\begin{bmatrix} i_s \\ \varphi_r \end{bmatrix} + \begin{bmatrix} B_1 \\ 0 \end{bmatrix} v_s$$
$$\frac{d}{dt}\begin{bmatrix} i_s \\ \varphi_r \end{bmatrix} = Ax + Bv_s \tag{36}$$

$$i_s = cx \ \& \ i_s = \begin{bmatrix} i_{ds} i_{qs} \end{bmatrix}^T$$
$$i_s = \begin{bmatrix} i_{ds} i_{qs} \end{bmatrix}^T \tag{37}$$
$$\varphi_r = \begin{bmatrix} \varphi_{dr} \varphi_{qr} \end{bmatrix}^T \ \& \ v_s = \begin{bmatrix} v_{ds} v_{qs} \end{bmatrix}^T$$

where i_s—stator current, φ_r—rotor flux, and V_s—stator voltage.

$$A_{11} = -\left\{ \left\{ \frac{R_s}{\sigma L_s} \right\} + \frac{(1-\sigma)}{\sigma T_r} \right\} I = a_{r11} I$$
$$A_{12} = \frac{M}{\sigma L_s L_r} - \left\{ \frac{1}{r_r} I - \omega_r J \right\} I = a_{r12} I + a_{r12} J \tag{38}$$

$$A_{21} = \frac{M}{T_r} I = a_{r21} I$$
$$A_{22} = \left(-\frac{1}{T_r} \right) I + \omega_r J = a_{r22} I + a_{r22} J \tag{39}$$

$$B_1 = \frac{1}{\sigma L_S} I = b_1 I \tag{40}$$

where R_s, R_r—resistance of Stator and Rotor, L_s, L_r—self-inductance of Stator and rotor, σ—Leakage coefficient, T_r—Time constant for the rotor, and ω_r—angular velocity of the motor.

Speed Estimation Adaptation Schemes

Unknown parameters must be comprehended in the state observer equation when the speed sensor cannot be mounted. One solution for reckoning the state and unrecognized parameters together is an adaptive observer, as shown in Figure 15. This led to the inclusion of a compatible program for calculating the speed of the rotor in the matrix A*, the equation calculating together the current of stator and rotor flux.

$$\frac{d}{dt}x^* = Ax^* + Bvs + G(i_s^* - i_s) \tag{41}$$

where

v_s—input of the system;
x^*—estimated state vector;
i_s—stator current;
i_s^*—estimated stator current;
A and B are constant matrices;
G—observer gain matrix.
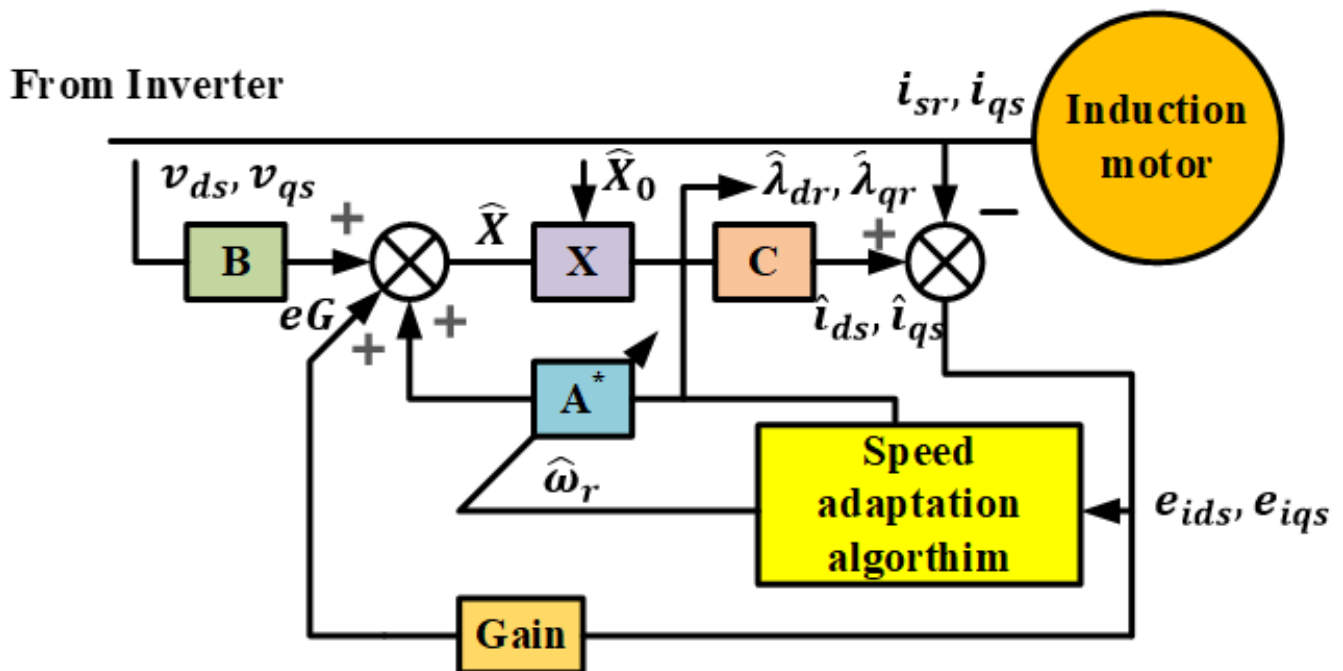
Figure 15. Adaptive flux observer.

An observer is an estimator that utilizes a plant scheme and a feedback model with an estimated plant variable. To devise a better method for estimating speed, the principal of a speed adaptive flux observer is used. Here, electrical model in a rotating reference frame is used by a full-order observer [74–76].

The rotor voltage equation is described by

$$R_r i_{dr}{}^s + \frac{d}{dt}\psi_{dr}{}^s + \omega_r \psi_{qr} \\ R_r i_{qr}{}^s + \frac{d}{dt}\psi_{qr}{}^s + \omega_r \psi_{dr} \tag{42}$$

$$\psi_{dr}{}^s = L_m i_{ds}{}^s + L_r i_{dr}{}^s \\ \psi_{qr}{}^s = L_m i_{qs}{}^s + L_r i_{qr}{}^s \tag{43}$$

From Equation (43),

$$i_{dr}{}^s = \frac{\psi_{dr} - L_m i_{ds}}{L_r} \\ i_{qr}{}^s = \frac{\psi_{qr} - L_m i_{qs}}{L_r} \tag{44}$$

Substitute $i_{dr}{}^s$ and $i_{qr}{}^s$ in Equations (42) and (43), respectively.

$$\begin{aligned}
\frac{d}{dt}\left(\psi_{dr}{}^s\right) &= -\frac{R_r}{L_r}\psi_{dr}{}^s - \omega_r\psi_{qr}{}^s + \frac{L_mR_r}{L_r}i_{ds}{}^s \\
\frac{d}{dt}\left(\psi_{qr}{}^s\right) &= -\frac{R_r}{L_r}\psi_{qr}{}^s - \omega_r\psi_{dr}{}^s + \frac{L_mR_r}{L_r}i_{qs}{}^s
\end{aligned} \tag{45}$$

$$\begin{aligned}
\frac{d}{dt}\left(\psi_{dr}{}^s\right) &= \frac{L_r}{L_m}V_{ds}{}^s - \frac{L_r}{L_m}\left(R_s + \sigma L_s{}^s\right)i_{ds}{}^s \\
\frac{d}{dt}\left(\psi_{qr}{}^s\right) &= \frac{L_r}{L_m}V_{qs}{}^s - \frac{L_r}{L_m}\left(R_s + \sigma L_s{}^s\right)i_{qs}{}^s
\end{aligned} \tag{46}$$

$$\begin{aligned}
\frac{d}{dt}\left(i_{ds}{}^s\right) &= -\frac{\left(L_m{}^2R_r + L_r{}^2R_s\right)}{\sigma L_s L_r{}^2}i_{ds}{}^s + \frac{\left(L_mR_r\right)}{\sigma L_s L_r{}^2}\psi_{dr}{}^s \\
&\quad + \frac{\left(L_m\omega_r\right)}{\sigma L_s L_r}\psi_{qr}{}^s + \frac{1}{\sigma L_s}V_{ds}{}^s
\end{aligned} \tag{47}$$

$$\begin{aligned}
\frac{d}{dt}\left(i_{qs}{}^s\right) &= -\frac{\left(L_m{}^2R_r + L_r{}^2R_s\right)}{\sigma L_s L_r{}^2}i_{qs}{}^s + \frac{\left(L_mR_r\right)}{\sigma L_s L_r{}^2}\psi_{qr}{}^s \\
&\quad - \frac{\left(L_m\omega_r\right)}{\sigma L_s L_r}\psi_{dr}{}^s + \frac{1}{\sigma L_s}V_{qs}{}^s
\end{aligned} \tag{48}$$

The desired state equation is calculated from the above equations and can be composed by the following equations. In the below figure * indicating the estimated values of the system.

$$\frac{d}{dt}(X) = Ax + Bvs$$

where,

$$\begin{aligned}
X &= \begin{bmatrix} i_{ds}{}^s & i_{qs}{}^s & \psi_{dr}{}^s & \psi_{qr}{}^s \end{bmatrix}^T \\
V_s &= \begin{bmatrix} V_{ds}{}^s & V_{qs}{}^s & 0 & 0 \end{bmatrix}^T
\end{aligned} \tag{49}$$

$$A = \begin{bmatrix}
-\dfrac{\left(L_m{}^2R_r + L_r{}^2R_s\right)}{\sigma L_s L_r{}^2} & 0 & \dfrac{\left(L_mR_r\right)}{\sigma L_s L_r{}^2} & \dfrac{\left(L_m\omega_r\right)}{\sigma L_s L_r} \\
0 & -\dfrac{\left(L_m{}^2R_r + L_r{}^2R_s\right)}{\sigma L_s L_r{}^2} & -\dfrac{\left(L_m\omega_r\right)}{\sigma L_s L_r} & \dfrac{\left(L_mR_r\right)}{\sigma L_s L_r{}^2} \\
\dfrac{L_mR_r}{L_r} & 0 & -\dfrac{R_r}{L_r} & -\omega_r \\
0 & \dfrac{L_mR_r}{L_r} & \omega_r & -\dfrac{R_r}{L_r}
\end{bmatrix}$$

The Lyapunov theorem is utilized to derive the adaptive scheme. The current of stator and rotor flux estimated error is implemented in Equation (50).

$$\frac{d}{dt}e = (A + GC)e - \nabla Ax^* \tag{50}$$

where

$$e = x - x^*$$

$$\nabla A = A^* - A = \begin{bmatrix} 0 & -\dfrac{\nabla\omega_r J}{C} \\ 0 & \nabla\omega_r J \end{bmatrix}, C = \frac{\sigma L_s L_r}{M}, \nabla\omega_r = \omega_r{}^* - \omega_r.$$

$$\begin{aligned}
\frac{d}{dt}v &= \left\{(A + GC)^T + (A + GC)\right\}e \\
&\quad - 2\nabla\omega_r\frac{\left(e_{ids}\varphi_{qr}{}^* - e_{iqs}\varphi_{dr}{}^*\right)}{C} \\
&\quad + 2\nabla\omega_r\frac{d}{dt}\frac{\psi_r{}^*}{\lambda}
\end{aligned} \tag{51}$$

$e_{ids} = i_{ds} - i_{ds}{}^* e_{iqs} = i_{qs} - i_{qs}{}^*$ from (51), by equating the second term to the third term, and the speed is estimated from the adaptive scheme

$$\frac{d}{dt}\psi_r = \frac{\lambda\left(e_{ids}\ \varphi_{qr}{}^* - e_{iqs}\ \varphi_{dr}{}^*\right)}{C} \tag{52}$$

The improved response of the speed estimation is calculated in Equation (53).

$$
\begin{aligned}
\psi_r{}^* = {}& K_p\left(e_{ids}\varphi_{qr}{}^* - e_{iqs}\varphi_{dr}{}^*\right) \\
&+ K_I \int \left(e_{ids}\varphi_{qr}{}^* - e_{iqs}\varphi_{dr}{}^*\right)dt
\end{aligned}
\tag{53}
$$

K_P, K_I is the positive gain of arbitrary.

Sliding Mode Observer

A reduced-order discrete time is used to reduce the estimation processing time. This took much less estimation time than a full-order observer in sliding mode. An extended version of the observer mentioned above is suggested for online evaluation of rotor flux, speed, and resistance of the rotor in an AC motor by using a robust closed-loop linearization control. However, there is a probability of a state space associate being included, which can lead to the mortification of the system [77–79]. This coupling occurs when there is a change in the resistance in the rotor. An online approximation of rotor flux, rotor resistance and speed is necessary. A sliding mode observer is suitable for attaining good dynamic performance only for a specific class of non-linear systems. When the upper bounds values of modeling in accuracies, disturbances and parameter variations are known, this controller design is accurate. Often, factors such as the selection of an untangle description of a dynamic system and ambiguity about the plant give rise to modeling inaccuracies. Hence, the systematic approach to the issue of retaining stability is provided by a sliding mode controller design. It is also capable of giving an adequate performance in the presence of modeling imperfection. For tracing the control of motors, whose mechanical load changes only an extensive range, sliding mode control is appropriate in such cases. Induction motors that proceed with complicated trajectories use induction motors as an activator for manipulating movements. The sliding mode controller is computationally simple compared to the adaptive controller and durable parameter changes. However, the unexpected and significant variation of variables under action often puts enormous pressure on the plant to be supervised. This can be counted as a disadvantage of sliding mode control. It also guides the plant states' rambling [80,81].

The estimator deviates the flux and speed from the actual values in the parameter. As a result, if any different from the present value, a new sliding mode adaptive scheme and flux observer is investigated to make flux and speed calculation rugged to parameter variation. In sliding mode, current observers are used in this method, by the communications of the two current sliding mode observers and the effect of parameter variation. On the rotor, the flux observer can be reduced. A special application of feedback linearization of non-linear systems is the diverse, dynamic technique, also known as the computed torque technique. A linear is a non-linear equation of robust motion by cancelling the same or all non-linear terms, and a commutated torque controller is used. This way, the feedback controller is made with linear to achieve the craved closed-loop performance. With a sliding mode, the system dynamics are controlled, giving system dynamics with variances property to uncertainties. To design a suitable sliding mode control, the first step is to choose a sliding surface capable of modeling the desired closed-loop achievements indifferent space. Then, model the design of control. It must be depicted in such a way so that plant state trajectories are mandatory towards the direction of the sliding surface, and they remain on it. The reaching phase is the period taken by the system state trajectory before reaching the sliding surface. The model trajectory attains the sliding region; it stays on it and subsequently moves along to the origin. The sliding mode is the system trajectory sliding along the sliding area [82].

The constraints in the induction motor for a controller design are delineated by the following equations:

$$
T_r = \frac{L_r}{R_r}, \sigma = 1 - \frac{L^2{}_m}{L_s L_r}, = \frac{L_m}{\sigma L_s L_r}, \gamma = \frac{R_s}{\sigma L_s} + \beta \frac{1}{T_r} L_m
$$

From the value of current and voltage signals, the expressions of back EMF can be observed as

$$
\begin{aligned}
e_{mq} &= V_{sq} - R_s i_{sq} - \sigma L_s \frac{d}{dt} i_{sq} \\
e_{md} &= V_{sd} - R_s i_{sd} - \sigma L_s \frac{d}{dt} i_{sd}
\end{aligned}
\tag{54}
$$

It is able to acquire the back-EMF equations is given by

$$
\begin{aligned}
e_{mq} &= L^* m \frac{d}{dt} i_{qm} \\
e_{md} &= L^* m \frac{d}{dt} i_{dm}
\end{aligned}
\tag{55}
$$

where $L^* m = \frac{L^2 m}{L_r}$.

The magnetizing currents are written by

$$
\begin{aligned}
i_{qm} &= \frac{L_r}{L_m} i_{rq} + i_{sq} \\
i_{dm} &= \frac{L_r}{L_m} i_{rd} + i_{sd}
\end{aligned}
\tag{56}
$$

The following equations calculate the magnetizing currents of differential equations

$$
\begin{aligned}
\frac{d}{dt} i_{qm} &= -\frac{1}{Tr} i_{qm} + p\omega_r i_{dM} + \frac{1}{T_r} i_{sq} \\
\frac{d}{dt} i_{dm} &= -\frac{1}{T_r} i_{dm} + p\omega_r i_{qm} + \frac{1}{T_r} i_{sd}
\end{aligned}
\tag{57}
$$

$$
\begin{aligned}
\frac{d}{dt} i_{qM} &= \frac{e_{mq}}{L^* m} \\
\frac{d}{dt} i_{dM} &= \frac{e_{md}}{L^* m}
\end{aligned}
\tag{58}
$$

Thus, Equation (53) helps to calculate the magnetizing current using the computed back EMF. These methods to obtain magnetizing currents are demonstrated by repressions, Equations (57) and (58). In the first technique, the currents of the stator and the data that include the rotor speed statistics are present. In contrast, magnetizing currents have been calculated personally from the back EMF in the second approach. To implement the first approach stated above, rotor speed information is needed. Without speed information, this method cannot be implemented. Observer depends on the sliding mode technique for the magnetizing current and can be used for the second method stated above, as it uses only voltage and current signals. The parameters to be obtained from the rotor speed information diagram for the sliding mode observer are given in Figure 16.

The extended state vector of reduced dimension for calculating the rotor time constant is observed by the X_{re} equation.

$$
X_{re} = \begin{bmatrix} \varphi_{dr} \varphi_{qr} \omega_r \sigma \end{bmatrix} = \begin{bmatrix} X_1 X_2 X_3 X_4 \end{bmatrix}^T
\tag{59}
$$

Extended Kalman Filter (EKF)

The sampled continuous EKF depends on the looping state, and data estimation are acceptable to manipulate with several input and non-linear output EKF, which should be adjusted to the noisy features of the estimated output by selecting the values in the covariance matrices using this matrix. The initial ambiguities in the calculated condition and parameters can also be tuned for an EKF, as shown in Figure 17. In [83–86], the procedure noise covariance matrix gives the freedom to use the version with actual interference in their states and models that are not proper in their formation. Knowledge of the mechanism that brings about the changes in state and parameter is not required. This paper presents a special booting of the procedure covariance matrix to enhance the fitter dynamics during start-up. To find the components of d-q and all manual parameters of an asynchronous motor, EKF is used. This is categorized as a reduce-order approach where a variable output equation is obtained. Considering the parameters of the ACmotor as secondarily stated, EKF can be analyzed for parameter and state findings. Moreover, it can be used for forming an augmented state vector. So, the inter-product of states, the nonlinear extended state

space model, is one irrespective of the accurate linear state space model. The non-linear expanded model is dealt with directly in EKF. The linearized model structure is around an operation point to give a linear perturbation structure to handle the EKF with the non-linear model. A sixth enlarged state space model with the exceeding state vector [87–89] is produced because of the advantages of EKF to the concurrent identifications of motor flux combined with motor parameters.

$$
\begin{aligned}
x_e(k) &= [x_e1(k) \ldots \ldots x_e6(k)]^T = [x1(k)x2(k)\theta1(k) \ldots \theta4(k)]^T \\
&= [\psi^r r_d(k) \psi^r r_q(k) \tau r^{-1}(k) L_s^*(k) L_m(k) R_s(k)]^T
\end{aligned}
\tag{60}
$$

where the subscript e indicates the increased state vector.

$$
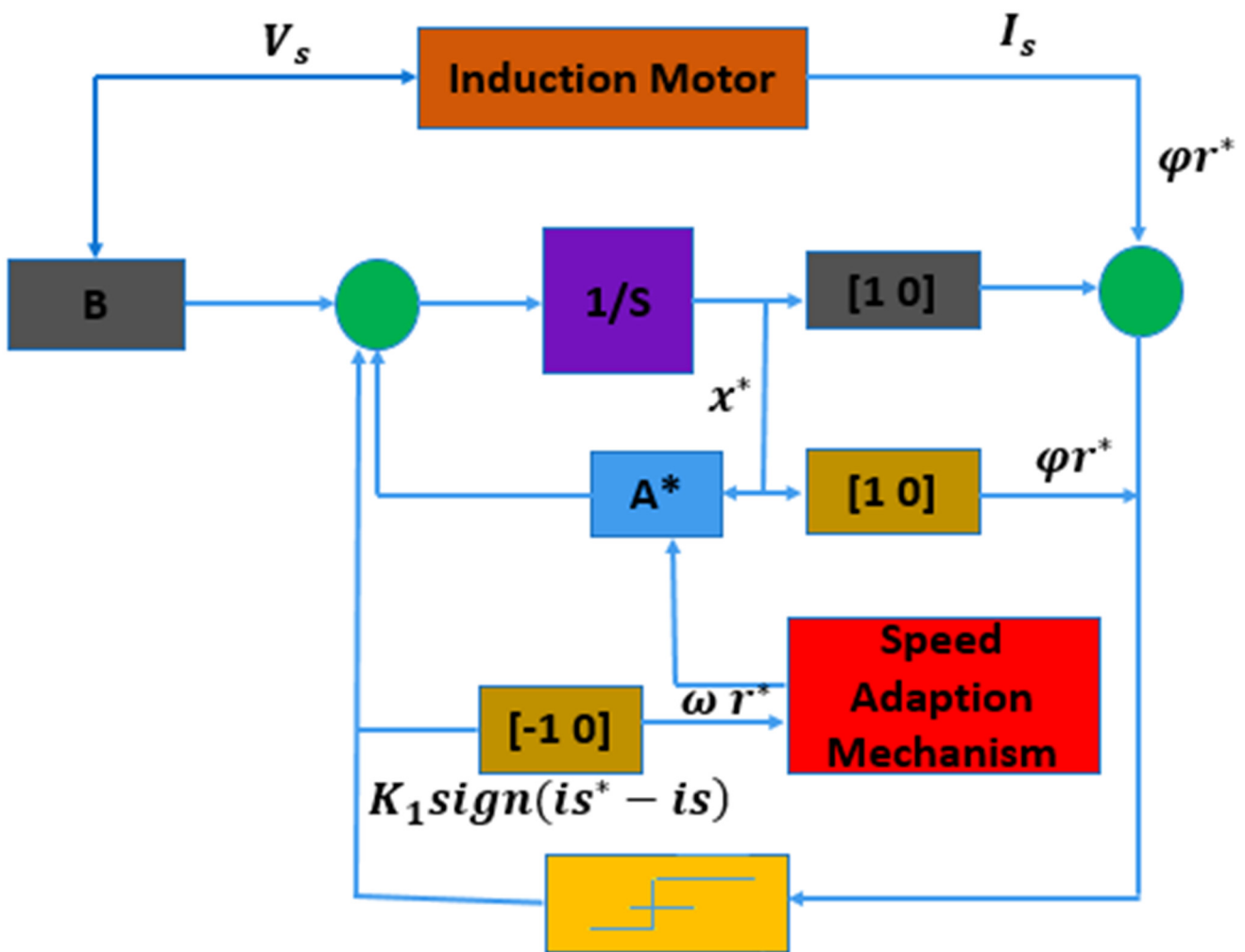\theta_j(k+1) = \theta_j(k) + r\theta_j(k)
\tag{61}
$$

Figure 16. Sliding mode observer.

Consider the state-space model of nonlinear stochastic discrete-time

$$
x_e(k+1) = f(x(k), u(k), \theta(k)) + r_{se}(k)
\tag{62}
$$

$$
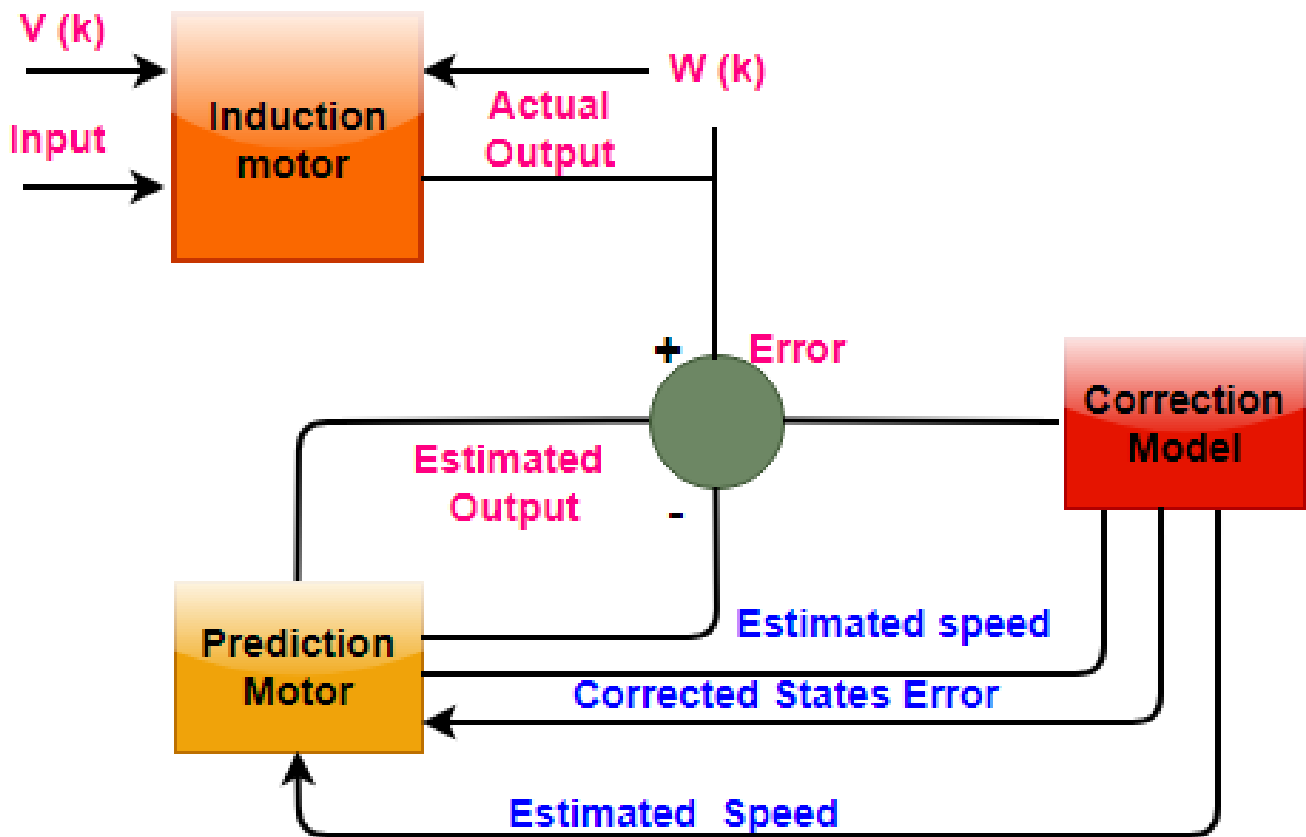y(k) = h(x(k), \theta(k)) + r_m(k) \& x_e(0) = x_e(x(0), \theta(0))
\tag{63}
$$

Figure 17. Extended Kalman filter.

The modelling of the extended Kalman filter can be demonstrated as follows:

$$
\begin{cases}
\{E(x(0)) = \hat{xe}(0) \\
E\left\{ \left(xe(0) - \hat{xe}(0)\right)\left(xe(0) - \hat{xe}(0)\right)^T = P(0)
\end{cases}
\tag{64}
$$

$$
\hat{xe} = (k+1/k) = f\left(\begin{array}{c} \hat{xk}/k, u(k), \dot{\hat{\theta}}(k/k)/1 \\ \theta(k) \end{array} \right) + \left(\begin{array}{c} rs(k) \\ r\theta(k) \end{array} \right)
$$
$$
= fe\left(\hat{xk}/k, u(k)\right) + res(k)
\tag{65}
$$

$$
F(k) = \frac{\frac{\partial fe(xe(k),u(k))}{\partial xe^T(K)}}{xe(k)} = \hat{xe}(k/k) =
$$
$$
\left[\begin{array}{cc} \frac{\partial fe(x(k),u(k),\theta(k))}{\partial x^T(K)} & \cdot \quad \frac{\partial fe(x(k),u(k),\theta(k))}{\partial x^T(K)}/\hat{xe}(k/k) \quad \cdot \\ 0 & I \end{array} \right]
\tag{66}
$$

$$
\hat{P}(k+1/k) = f(k)\hat{p}(k/k)F^T(K) + R(s)
\tag{67}
$$

$$
H(k) = \frac{\frac{\partial he(xe(k))}{\partial xe^T(K)}}{\hat{xe}\left(\frac{k+1}{k}\right)} =
$$
$$
\left[\begin{array}{ccc} \frac{\partial h(x(k),\theta(k))}{\partial x^T(K)} & \frac{\partial h(x(k),\theta(k))}{\partial x^T(K)}. & \frac{\partial h(x(k),\theta(k))}{\partial x^T(K)}/\hat{xe}\left(\frac{k+1}{k}\right) \quad \cdot \\ & \cdot & \cdot \end{array} \right]
\tag{68}
$$

$$
K(k+1) = \hat{p}(k+1/k)H^T(K)\left[H(k) P(k+1)/kH^T(k) + Rm\right].^{-1}
$$
$$
\hat{y}(k+1) = h\left(\hat{xe}(k+1/k), k\right)
\tag{69}
$$

$$\hat{xe}(k+1/k+1) = \hat{xe}(k+1/k) + K(k+1)\left[y(k+1) - \hat{y}(k+1)\right]$$

$$\hat{P}(k+1/k+1) = [I - K(k+1)H(K)]\hat{P}(k+1/k)$$

(70)

The above modeling is incorporated in the matlab for analyzing the behaviours of the machine by kalman filter methods Concurrent identifications of states and parameters are allowed by the extended Kalman filter. In an augmented state vector, these data are assumed as different states. Since the multiplication of states takes place now, the augmented model results are non-linear. Thus, to obtain a linear perturbation model, the state trajectory must be linearized to handle the extended Kalman filter algorithm; the discrete condition AC motor model is accented in the rotating and d-q frame of reference.

Model Reference Adaptive System (MRAs)

One of the generally used drives is the speed sensorless drive approach, the MRAs. In the MRAS, two models are present, which perform parallel as shown in Figure 18 and simulation model is illustrated in Figure 19. The first model is the valuation of the induction motor's flux linkage, named as a reference model, and the potential difference between two points and currents are input. The output flux linkage of the induction motor of this model was studied as unstable [90–93].

$$\psi_{dr} = \frac{L_r}{L_m} \int [V_{ds} - R_s\, i_{ds}]dt$$
$$- \left[L_s - \frac{L^2m}{L_m}\right] i_{sd}$$

(71)

$$\psi_{qr} = \frac{L_r}{L_m} \int [V_{qs} - R_s i_{qs}]dt$$
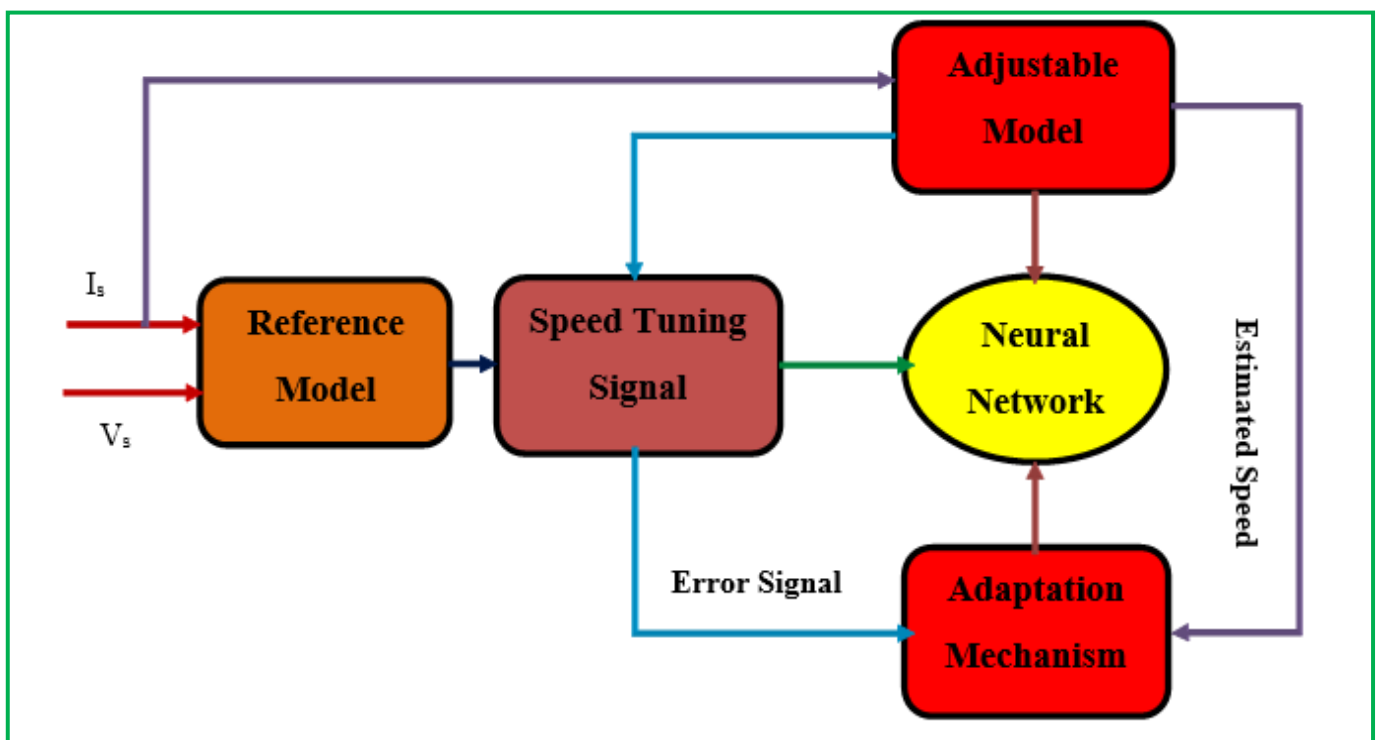$$- \left[L_s - \frac{L^2m}{L_m}\right] i_{sq}$$

(72)

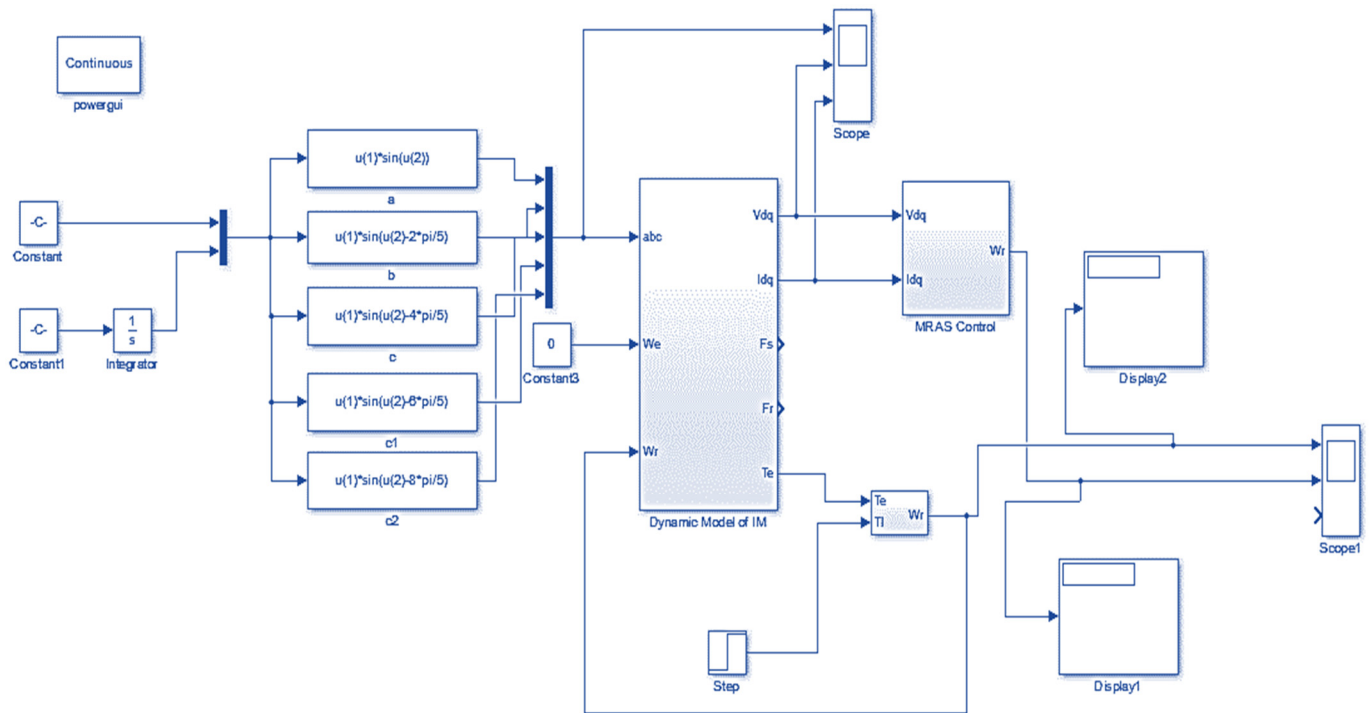**Figure 18.** Model reference adaptive system and control.

Figure 19. Simulink model of MRAS control.

Equations (71) and (72) represent a voltage model for the stator. These have not had the speed of a rotor and are, accordingly, a model. The induction motor rotating voltage equations contain the rotor flux and the speed when they are stated in a stationary reference frame [94–96]. Equations of the adaptive model are

$$\psi_{dr} = \frac{1}{T_r} \int [L_m i_{ds} - \omega_r T_r \psi_{qr}{}^* - \psi dr^*] dt \tag{73}$$

$$\psi_{qr} = \frac{1}{T_r} \int [L_m i_{qs} - \omega_r T_r \psi_{dr}{}^* - \psi_{qr}{}^*] dt \tag{74}$$

The reference and adjustable models are considered to figure out the angular difference and the flux linkages of the rotor's outputs of the two estimators. The reference and adjustable model are tuned using an adaptation mechanism with the controller until the error state reaches zero value [97–101].

Model Reference Adaptive System with Soft Computing Technique

An input and output model is there for the MRAS depending on the approach depicted in the preceding section. However, if a neural network partly exchanges the statistical approach, greater exactness and robustness can be obtained. A separate PI controller can be employed this way since this can be interspersed into the neural network-based adaptive device. An ANN on a fuzzy neural network is some of the frames of the neural network-based model. The adjustable model has been exchanged by a two-layer ANN. However, the input prototype is still needed to determine the motor flux, which is taken as a speed adapting signal. Several machine parameters, such as Rs and Ls, are used to construct the previous input model. These data may vary their values during a motor performance for different periods. The value of these parameters is also constant in the input model. Hence, even at a motor low-speed running period, ANN speed estimation is very sensitive to parameter deviations. A resistance of stator estimator is applied in the new input model to rectify the above problems and form the project more commercial of the machine data. In

this, the resistance of the stator (Rs) value could be measured online [102–104]. The survey for parameter estimation by online identification methods is listed in Table 3.

Table 3. Survey for parameter estimation by online identification methods.

Recognition Method	Recognition Principle	Recognition Parameters	Benefits	Limitations
Kalman filter extended	Motor state equation used directly.	Resistance of rotor, mutual inductance.	The effect of filtering is good. It has high precision time and reduced interference.	High processor required; calculation is difficult.
MRAS	The exact operating condition of the motor is a reference model. The state equation of the motor is a flexible model then the controller prosed the error value between these models.	Resistance of stator and rotor.	Less calculation time.Very high precisions.	Determination of the reference model is challenging.
Intelligent technique	A fuzzy logic controller, neural network, adaptive neural network, and genetic algorithm is considered in this technique.	Inductance and resistance.	Precise and reliable.	Very high processor is also needed computation time is difficult.

5. Hardware Results and Discussions

Every stator coil testing is executed independently. Hence, in the instance of capacitance initiate electric drive, the electrical condenser is ignored. To move from the plugged rotor testing, stator and primary coils are carried out independently. Although, in each instance, the transmitted voltage, electric current and energy is determined. Moreover, the fast electric connection is to avert and to warm. An appropriate termination has been employed. An evaluated potential is selected to carry out without a load test. If the significant coil is considered, then the estimations of the transmitted potential, electric current and intensity are required. Thus, the way of winding exposure and friction damage examination is held. The transmitted intensity gain that offers friction damage and winding damage is determined. The hardware setup for parameter estimation is depicted in Figure 20.
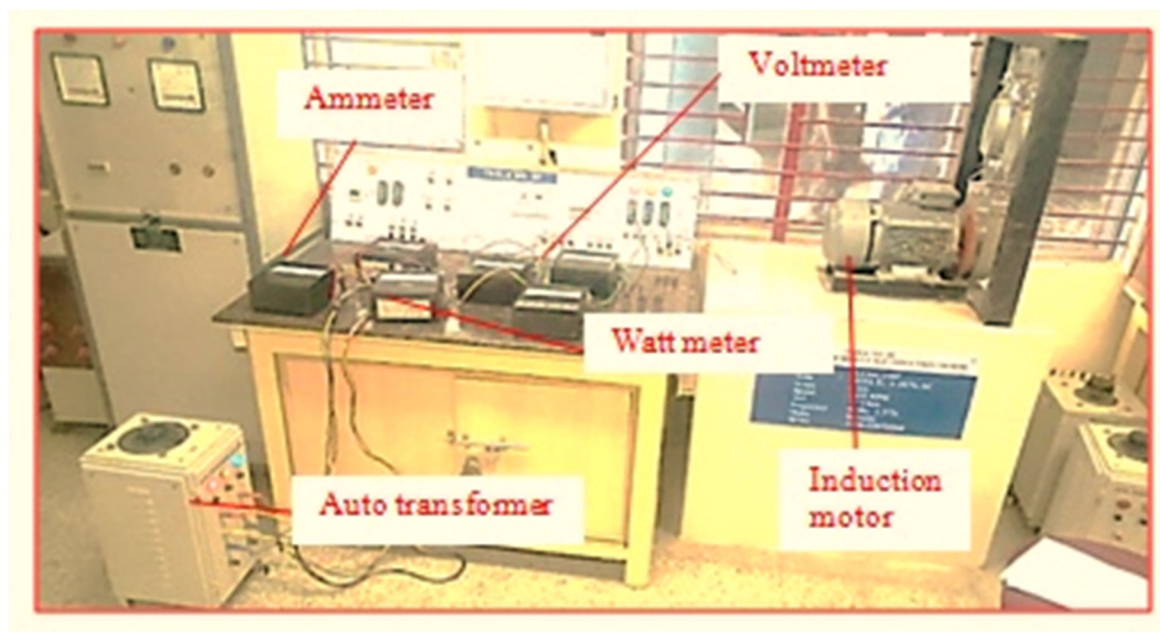

Figure 20. The hardware setup for parameter estimation.

From the parameter estimation techniques, the modified, extended Kalman filter performs better than the other methods, as depicted in Table 4. However, this method is difficult for hardware implementation due to the noise factor of EKF. The modified MRAS technique has comparable performance to the Kalman filter. The proposed MRAS technique is a simple method for hardware implementation.

Table 4. Numerical analysis for speed estimation techniques.

Estimation Technique	Rise Time (s)	Settling Time (s)	Delay Time (s)	Steady State Error (%)	Peak Overshoot
modified model reference adaptive system	0.989	0.989	0.89	0	0
modified luenberger observer method	1.4	2.00	1.34	8.8	6.8
the modified, extended Kalman filter method	0.05	0.2	0.38	0	3.14
conventional model reference adaptive system	2.200	1.9	1.72	2.89	8.9
conventional luenberger observer method	1.95	2.888	2.3	11.899	8.99
conventional extended Kalman filter method	1.488	1.100	1.00	2.12	4.954

The speed performance is analyzed for no load, balanced load and unbalanced load conditions from the induction motor drive hardware implementation, as shown in Tables 5–7, respectively.

Table 5. Speed performance in no load condition.

Voltage (V)	Current (A)	Speed (RPM)
40	2	1220
85	2.4	1482
110	2.3	1480
135	2.3	1480
210	2.1	1482
360	2.4	1486
420	3.5	1486

Table 6. Speed performance in balanced load condition.

Voltage (V)	Current (A)	Load (Kg)	Speed (RPM)
400	2.102	2.48	1486
400	2.488	4.88	1480
400	3.128	11	1490

Table 7. Speed performance in unbalanced load condition.

Voltage (V)	Current (A)	Load (Kg)	Speed (rpm)
400	2.111	Motor 1—2.5 Motor 2—no load	Motor 1—1460 Motor 2—1480
400	2.499	Motor 1—3 Motor 2—1	Motor 1—1425 Motor 2—1480

From Table 5, it is shown that the speed deviation is minimal for wide variations of voltage at no load conditions. Variable Speed control is difficult due to the absence of a power electronics converter. In the performance of two induction motors connected in parallel with balanced load conditions, the speed of two different motors is almost the same and is shown in Table 6.

Under unbalanced load conditions, the speed deviation becomes high, which is depicted in Table 7. To rectify the problem mentioned above, the two-level voltage source inverter feeding parallel connected induction motors is tested using the DTC-SVM-based control technique.

6. Conclusions

Induction motor usage in industries has increased dramatically, as it offers several advantages, such as reliability, low cost and robustness. However, regularly monitoring its parameters, such as speed control and torque control, is required to help the motor match its advantages. It determines the electrical system's performance during dynamic and steady operating conditions as the motor operates in a wide range of parameters. The various parameter estimation techniques and dynamic modeling of induction motors have been reviewed. Moreover, the simulation of a dynamic model of an asynchronous motor and MRAS also verified the system's performance. This paper presents a simple and effective solution that provides the platform for modeling and parameter estimations through the above derivations and study. Induction motor monitoring is the process of identifying a motor's defects. An induction motor experiences issues such as over-voltage, above-rated current, high temperature, higher-than-rated speed, and high circulating bearing current while it is in operation. The understanding of an induction motor drive system at high circulating current circumstances becomes crucial from the perspectives of improved system design, sanctuary, and fault-unbiased control. The behavior of induction motors under parameter modification settings was a fundamental and difficult problem for electrical researchers. Common mode voltage results in common mode current, which causes a variety of issues in industrial electrical systems that may result in damage at the output terminal.

This results in damage to motor bearings, which could lead to malfunctioning machines and unwanted tripping of relays. It has been observed that the main cause of motors' faults and bearings is this common mode voltage. AC motors' finite element realization and signal processing approach is essential in stable and faulty situations.

7. Observations

Dynamic induction models based on Simulink are available in several books and research papers. However, these models are described as a black box with no inside relationship accurate in the available text matter. Some of these texts have recommended using purpose for approaching the model data, but they are not feasible as they do not use the Simulink at full power and capacity. Even though the s function runs faster than discrete Simulink blocks, it is still possible to make them faster using an accelerator or non-linearity model. The available machine's model permits the complete formation of the model equations of Simulink structure, so it is reproduced in an aspect that makes it easy for the reader to develop and recognize. The problem can also be easily solved by employing an offline motor. The online identification of a synchronous motor is required to monitor the motor's precision. In several cases, it happens such that, not only these kinds of experimental conditions are tough to achieve but also very uneasy about installing and removing the load on the system. Apart from this, the skin effect of the rotor is also a severe concern.

- In the no-load experiment method, recognition accuracy is not significant, and the rotor circuit is not taken into consideration. To No load, a removed load is not a very convenient process.
- The auto-tuning method can be utilized in the closed-loop setup with a frequency converter. However, using the same in the closed loop setup without a frequency converter is uncomfortable.

- The high rating and experimental data, on the whole, need to be computed in the least square method. However, the measurement and calculation of this experimental data is a tedious process/task.
- In an extended Kalman filter, a high processor is required, and the computation time for the algorithm is too high. The processor requirement is high, and intelligent algorithms are also tricky. The offline identification method is subdivided into many classes.
- The least square method is an improved method for systems requiring high understanding accuracy, less cost, accurate achievement, and easy application. This method is performed because it realizes not only offline understanding but also online understanding. The control system is a type of system that requires very high precision of understanding.

Abbreviations

V_a, V_b, V_c	Line voltages of three-phase induction motor
V_{sd}	Voltage of Stator for d-axis
V_{sq}	Voltage of Stator for q-axis
V_{rd}	Voltage of Rotor for d-axis
V_{rq}	Voltage of Rotor for q-axis
i_{sd}	Current of Stator for d-axis
i_{sq}	Current of Rotor for q-axis
i_{rd}	Current of Rotor for d-axis
i_{rq}	Current of Rotor for q-axis
R_s	Resistance of stator
R_r	Resistance of rotor
ω_d	Reference frame of angular velocity
$\lambda_{sd}, \lambda_{sq}$	Stator flux linkages
$\lambda_{rd}, \lambda_{rq}$	Rotor flux linkages
L_r	Self-inductance of the rotor
L_s	Self-inductance of the stator
L_m	Magnetizing inductance
L_{lr}	Leakage inductance of rotor
L_{ls}	Leakage inductance of stator
D	Direct axis
Q	Quadrature axis
S	Variable of the stator
R	Variable of rotor
P	Number of poles
Te	Electromagnetic torque
DC	Direct current
MRAS	Model reference adaptive system
SVPWM	Space vector pulse width modulation (SVPWM)
PLC	Programmable logic controller (PLC)
MCSA	Motor current signature analysis
VSD	Variable speed drives
STFT	Short-time Fourier transforms
DSP	Digital signal processor
RFO	Rotor flux oriented
IM	Induction motor
FOC	Field oriented control

References

1. Reddy, G.S. Vector Controller based Speed Control of Induction Motor Drive with 3-Level SVPWM based Inverter. *Int. J. Emerg. Trends Electr. Electron.* **2013**, *1*, 1–11.
2. Dabbeti, S.; Lakshmi, K.V. Sensorless Speed Control of an Induction Motor Drive using Predictive Current and Torque Controllers. *Adv. Electron. Electr. Eng.* **2013**, *3*, 1177–1196.
3. Suwankawin, S.; Sangwon, S. A Speed-Sensorless IM Drive with Decoupling Control and Stability Analysis of Speed Estimation. *IEEE Trans. Ind. Electron.* **2002**, *49*, 444–455. [CrossRef]
4. Rassolkin, A.; Kallaste, A.; Orlova, S.; Gevorkov, L.; Vaimann, T.; Belahcen, A. Re-Use and Recycling of Different Electrical Machines. *Latv. J. Phys. Tech. Sci.* **2018**, *55*, 13–23. [CrossRef]
5. Usha, S.; Subramani, C.; Padmanaban, S. Neural Network-Based Model Reference Adaptive System for Torque Ripple Reduction in Sensorless Poly Phase Induction Motor Drive. *Energies* **2019**, *12*, 920. [CrossRef]
6. Panchal, M.S.N.; Sheth, M.V.S.; Pandya, M.A.A. Simulation Analysis of SVPWM Inverter Fed Induction Motor Drives. *Int. J. Emerg. Trends Electr. Electron.* **2013**, *2*, 18–22.
7. Haq, H.; Imran, M.H.; Okumu, H.I.B. Speed Control of Induction Motor using FOC Method. *Int. J. Eng. Res. Appl.* **2015**, *5*, 154–158.
8. Matsuse, G.K.; Kouno, Y.; Kawai, H.; Oikawa, J. Characteristics of speed sensorless vector controlled dual induction motor drive connected in parallel fed by a single Inverter. *IEEE Trans. Ind. Appl.* **2004**, *40*, 153–161. [CrossRef]
9. Gunabalan, R.; Subbiah, V. Stability Analysis of Single Inverter Fed Two Induction Motors in Parallel. *World Academy of Science Eng. Technol.* **2014**, *8*, 1316–1320.
10. Yoshinaga, T.; Terunuma, T.; Matsuse, K. Basic characteristic of parallel connected dual induction motor drives with matrix converter. In Proceedings of the 34th Annual Conference of IEEE Industrial Electronics, Orlando, FL, USA, 10–13 November 2008; pp. 584–589.
11. Ojha, S.; Pandey, A.K. Close Loop V/F Control of Voltage Source Inverter using Sinusoidal PWM, Third Harmonic Injection PWM and Space Vector PWM Method for Induction Motor. *Int. J. Power Electron. Drive Syst.* **2016**, *7*, 217–224. [CrossRef]
12. Adiuku, C.O.; Beig, A.R.; Kanukollu, S. Sensorless Closed Loop V/F control of medium-Voltage High-Power Induction Motor with Synchronized Space Vector PWM. *IEEE Trans. Ind. Appl.* **2015**, 784–799. [CrossRef]
13. Rahman, A. Three-phase induction motor design optimization using the modified Hooke-Jeeves method. *Int. J. Electr. Mach. Power Syst.* **1990**, *18*, 1–12.
14. Dehkordi, B.M.; Kiyoumarsi, A.; Ashrafi, R. Optimal Design of a Soft Switching Inverter for Control of an Induction Motor Drive Using Scalar Method. In Proceedings of the International Conference on Electrical Machines, Wuhan, China, 6–9 September 2008.
15. Thakur, P. Simulation of Soft-Switched Three-Phase Inverter for RL and Induction Motor Load. *Int. J. Eng. Res. Technol.* **2014**, *3*, 2408–2416.
16. da Silva, E.R.; Cavalcanti, M.C.; Jacobina, C.B. Comparative study of pulsed DC-link voltage converters. *Power Electron. Spec. Conf.* **2000**, *2*, 1035–1040.
17. Behera, S.; Das, P.; Doradla, S.R. Quasi-resonant inverter-fed direct torque controlled induction motor drives. *Electr. Power Syst. Res.* **2007**, *77*, 946–955. [CrossRef]
18. Benbouzid, M.; Vieira, M.; Theys, C. Induction motor's fault detection and localization using stator current advanced signal processing techniques. *IEEE Trans. Power Electron.* **1999**, *14*, 14–22. [CrossRef]
19. Tandon, N.; Yadava, G.S.; Ramakrishna, K.M. A comparison of some condition monitoring techniques for the detection of defect in induction motor ball bearings. *Mech. Syst. Signal Process.* **2007**, *21*, 244–256. [CrossRef]
20. Siddique, A.; Yadava, G.S.; Singh, B. A review of stator fault monitoring techniques of induction motors. *IEEE Trans. Energy Convers.* **2005**, *20*, 106–114. [CrossRef]
21. Ioannides, M.G. Design and implementation of PLC-based monitoring control system for induction motor. *IEEE Trans. Energy Convers.* **2004**, *19*, 469–476. [CrossRef]
22. Mousavi, S.M. Dash.Application of Speed Estimation Techniques for Induction Motor Drives in Electric Traction Industries and vehicles. *Int. J. Automot. Eng.* **2014**, *4*, 857–867.
23. Thomson, W.T.; Fenger, M. Current signature analysis to detect induction motor faults. *IEEE Ind. Appl. Mag.* **2001**, *7*, 26–34. [CrossRef]
24. Ahuja, P.; Kumar, R.; Dhiraj, K. Control and Monitoring of 3 Phase Induction Motor Using PLC. *Int. J. Innov. Res. Sci. Eng. Technol.* **2016**, *5*, 1225–1229.
25. Cabal-Yepez, E.; Fernandez-Jaramillo, A.A.; Garcia-Perez, A.; Romero-Troncoso, R.J.; Lozano-Garcia, J.M. Real-time condition monitoring on VSD-fed induction motors through statistical analysis and synchronous speed observation. *Int. Trans. Electr. Energy Syst.* **2015**, *25*, 1657–1672. [CrossRef]
26. Siddharth, U, Comparative analysis between proportional integral controller and wavelet controller for the fault detection in induction motor. *Int. J. Thesis Proj. Diss.* **2013**, *1*, 17–44.
27. Sridhar, R.; Vishnuram, P.; Sattianadan, D. Efficient Single Stage Photovoltaic Pumping System Using BLDC Motor with Grid Power Export. *ASME. J. Sol. Energy Eng.* **2019**, *141*, 051004. [CrossRef]
28. Faiz, J.; Shahgholian, G. Modeling and Simulation of a Three-Phase Inverter with Rectifier-Type Nonlinear Loads. *Armen. J. Phys.* **2009**, *2*, 307–316.

29. Krause, P.C.; Thomas, C.H. Simulation of Symmetrical Induction Machinery. *IEEE Trans. Power Appar. Syst.* **1965**, *84*, 1038–1053. [CrossRef]

30. Punit, L.; Ratnani, A.G. ThosarMathematical Modelling of a 3 Phase Induction Motor Using MATLAB/Simulink. *Int. J. Mod. Eng. Res.* **2014**, *4*, 62–67.

31. Hatos, A.F.P. Parameter sensitivity analysis of an induction motor. *Hung. J. Ind. Chem.* **2011**, *39*, 157–161.

32. Dorjsuren, Y.; Tumenbayar, L.; Tsevegmid, J. Three-axis dynamic modeling of induction motor. *Int. J. Math. Models Methods Appl. Sci.* **2015**, *9*, 527–536.

33. De la Barrera, P.M.; Bossio, G.R.; Solsona, J.A.; García, G.O. Model for three-phase induction motors with stator core faults. *IET Electric Power Appl.* **2010**, *4*, 591–602. [CrossRef]

34. Zanganeh, M.; Roknabadi, H.A. Modeling and Simulation and Analysis of Three-Phase Squirrel-Cage Induction Motors Behavior in the Conditions of Types of Short Circuit in the Stator Terminal. *Indian J. Fundam. Appl. Life Sci.* **2014**, *4*, 601–611.

35. Ayasun, S. Induction motor test using MATLAB/Simulink and their Integration into Undergraduate Electric Machinery courses. *IEEE Trans.* **2005**, *48*, 37–46. [CrossRef]

36. Phanindrakumar, P.N.H.; Deshpande, D.M.; Dubey, M. Modeling of Vector Controlled Induction Motor in Different Reference Frames. *Int. J. Innov. Res. Sci. Eng. Technol.* **2014**, *3*, 71–78.

37. Leedy, A.W. Simulink/MATLAB Dynamic Induction Motor Model for Use as a Teaching and Research Tool. *Int. J. Soft Comput. Eng.* **2013**, *3*, 102–107.

38. Autsou, S.; Rassõlkin, A.; Gevorkov, L.; Saroka, V.; Karpovich, D.; Vaimann, T.; Kallaste, A.; Belahcen, A. Comparative Study of Field-OrintedContol Model in Application for Induction and Synchronous Reluctance Motors for Lifecycle Analysis. In Proceedings of the 25th International Workshop on Electric Drives: Optimization in Control of Electric Drives IWED, Moscow, Russia, 31 January–2 February 2018.

39. Slemon, G.R. Modelling of Induction Machines for Electric Drives. *IEEE Trans. Ind. Appl.* **1989**, *25*, 1126–1131. [CrossRef]

40. Lekhchine, S.; Bahi, T.; Aadlia, I.; Layate, Z. Speed control of doubly fed induction motor. *Sci. Direct Procedia* **2015**, *74*, 575–586. [CrossRef]

41. Gupta, S.; Wadhwani, S. Dynamic Modeling of Induction Motor Using Rotor Rotating Reference Frame. *Int. J. Adv. Res. Electr. Electron. Instrum. Eng.* **2014**, *3*, 10132–10140.

42. Saidur, R.; Mekhilef, S.; Ali, M.B.; Safari, A.; Mohammed, H.A. Applications of variable speed drive (VSD) in electrical motors energy savings. *Renew. Sustain. Energy Rev.* **2012**, *16*, 543–550. [CrossRef]

43. Ibrahim, M.; Alsofyani, N.R.; Idris, N. A review on sensorless techniques for sustainable reliability and efficient variable frequency drives of induction motors. *Renew. Sustain. Energy Rev.* **2013**, *24*, 111–121.

44. Krishnan, R. *Electric Motor Drives Modeling, Analysis and Control*; PHI Learning Private Limited: New Delhi, India, 2001; pp. 492–501.

45. Bose, B.K. *Modern Power Electronics and AC Drives*; Prentice Hall: Upper Saddle River, NJ, USA, 2001; p. *348* 2350.

46. Soe, N.; Yee, T.H.; Aung, S.S. Dynamic Modeling and Simulation of Three phase Small Power Induction Motor. *World Acad. Sci. Eng. Technol.* **2015**, *18*, 421–424.

47. Batool, M.; Ahmad, A. Mathematical modeling and speed torque analysis of three phase squirrel cage induction motor using matlab Simulink for electrical machines laboratory. *Int. Electr. Eng. J.* **2013**, *4*, 880–889.

48. Bellure, A.; Aspalli, M.S. Dynamic d-q Model of Induction Motor Using Simulink. *Int. J. Eng. Trends Technol.* **2015**, *24*, 252–257. [CrossRef]

49. Wade, S.; Dunnigan, M.W.; Williams, B.W. Modeling and simulation of induction machine vector control with rotor resistance identification. *IEEE Trans. Power Electron.* **1997**, *12*, 495–506. [CrossRef]

50. Mariethoz, S.; Domahidi, A.; Morari, M. High-Band width Explicit Model Predictive Control of Electrical Drives. *IEEE Trans. Ind. Appl.* **2012**, *48*, 1980–1992. [CrossRef]

51. Ozpineci, B.; Tolbert, L.M. Simulink Implementation of Induction Machine Model-A Modular Approach. In Proceedings of the IEEE International Electric Machines and Drives Conference (IEMDC), Madison, WI, USA, 1–4 June 2003; pp. 728–734.

52. Shah, S.; Rashid, A.; Bhatti, M.K.L. Direct Quadrate (D-Q) Modeling of 3-Phase Induction Motor Using Matlab/Simulink. *Can. J. Electr. Electron. Eng.* **2012**, *3*, 237–243.

53. Toliyat, H.A.; Levi, E.; Raina, M. A Review of RFO Induction Motor Parameter Estimation Techniques. *IEEE Trans. Energy Convers.* **2003**, *18*, 271–283. [CrossRef]

54. Gastli, A. Identification of induction motor equivalent circuit parameters using the single-phase test. *IEEE Trans. Energy Conv.* **1999**, *14*, 51–56. [CrossRef]

55. Seok, J.K. Induction motor parameter tuning for high performance drives. *IEEE Trans. Ind. Appl.* **2001**, *37*, 35–41. [CrossRef]

56. Levi, E. Method of magnetizing curve identification in vector controlled induction machines. *Europe Trans. Elect. Power* **1992**, *2*, 309–314. [CrossRef]

57. Castaldi, P.; Tilli, A. Parameter Estimation of Induction Motor at Standstill with Magnetic Flux Monitoring. *IEEE Trans. Control. Syst. Technol.* **2005**, *13*, 386–400. [CrossRef]

58. Pandey, K.K.; Zope, P.H. Estimating Parameters of a Three-Phase induction motor using Matlab/Simulink. *Int. J. Sci. Eng. Res.* **2013**, *4*, 425–443.

59. Stephan, J.; Bodson, M.; Chiasson, J. Real-time estimation of the parameters and fluxes of induction motors. *IEEE Trans. Ind. Appl.* **1994**, *30*, 746–759. [CrossRef]

60. Kim, K.-Y.; Byun, S.-H. Auto-Measurement of Induction Motor Parameters. *J. Electr. Eng. Technol.* **2006**, *1*, 226–232. [CrossRef]
61. Khambadkone, A.M.; Holtz, J. Vector controlled induction motor drive with a self-commissioning scheme. *IEEE Trans. Ind. Appl.* **1991**, *38*, 322–327. [CrossRef]
62. Sengamalai, U.; Chinnamuthu, S. An experimental fault analysis and speed control of an induction motor using motor solver. *J. Electr. Eng. Technol.* **2017**, *12*, 761–768. [CrossRef]
63. Kerkman, R.J.; Thunes, J.D.; Rowan, T.M.; Schlegel, D.W. A frequency based determination of transient inductance and rotor resistance for field commissioning purposes. *IEEE Trans. Ind. Appl.* **1996**, *32*, 577–584. [CrossRef]
64. Nguyen, T.D.; Lee, H.H. Modulation strategies to reduce common-mode voltage for indirect matrix converters. *IEEE Trans. Ind. Elec.* **2012**, *59*, 129–140. [CrossRef]
65. Bharatiraja, C.; Selvaraj, R.; Chelliah, T.R.; Munda, J.L.; Tariq, M.; Maswood, A.I. Design and Implementation of Fourth Arm for Elimination of Bearing Current in NPC-MLI-Fed Induction Motor Drive. *IEEE Trans. Ind. Appl.* **2018**, *54*, 745–754. [CrossRef]
66. Holtz, J.; Thimn, T. Identification of the machine parameters in a vector-controlled induction motor drive. *IEEE Trans. Ind. Appl.* **1991**, *27*, 1111–1118. [CrossRef]
67. Finch, W.J.; Gauri, D. Controlled AC Electrical Drives. *IEEE Trans. Ind. Electron.* **2008**, *55*, 481–491. [CrossRef]
68. Shaw, S.R.; Leeb, S.B. Identification of Induction Motor Parameters from Transient Stator Current Measurements. *IEEE Trans. Ind. Electron.* **1999**, *46*, 139–149. [CrossRef]
69. Canakoglu, A.I.; Yetgin, G.H.T.; Turan, M. Induction motor parameter estimation using metaheuristic methods. *Turk. J. Electr. Eng. Comput. Sci.* **2014**, *22*, 1177–1192. [CrossRef]
70. Babarinde, A.K.; Adefarati, T.; Oluwole, A.S.; Kelechi, G.; Kehinde, I. Effects of Electrical Parameters Variation on The Dynamic Behaviour of two Phase Induction Motor. *Int. J. Eng. Sci. Invent.* **2014**, *3*, 15–25.
71. Kubota, H.; Matsuse, K.; Nakmo, T. DSP-Based Speed Adaptive Flux Observer of Induction Motor. *IEEE Trans. Ind. Appl.* **1993**, *29*, 344–348. [CrossRef]
72. Castaldi, P.; Geri, W.; Montanari, M.; Tilli, A. A new adaptive approach for on-line parameter and state estimation of induction motors. *Control. Eng. Pract.* **2005**, *13*, 81–94. [CrossRef]
73. Fang, C.H.; Lin, S.K.; Wang, S.J. On-line parameter estimator of an induction motor at standstill. *Control. Eng. Pract.* **2005**, *13*, 535–540. [CrossRef]
74. Alamir, M. Sensitivity analysis in simultaneous state/parameter estimation for induction motors. *Int. J. Control Eng.* **2002**, *75*, 753–758. [CrossRef]
75. Kubota, H.; Matsuse, K. Speed sensorless field oriented control of induction motor with rotor resistance adaptation. *IEEE Trans. Ind. Appl.* **1994**, *30*, 1219–1224. [CrossRef]
76. Tursini, M.; Petrella, R.; Parasiliti, F. Adaptive sliding-mode observer for speed-sensorless control of induction motors. *IEEE Trans. Ind. Appl.* **2000**, *36*, 1380–1387. [CrossRef]
77. Aydeniz, M.G.; Ibrahim, S.E. Luenberger-sliding mode observer with rotor time constant parameter estimation in induction motor drives. *Turk. J. Electr. Eng. Comp Sci.* **2011**, *19*, 901–912. [CrossRef]
78. Kim, D.I.; Ha, I.J.; Ko, M.S. Control of Induction Motors via Feedback Linearization with Input-Output Decoupling. *Int. J. Control* **1989**, *51*, 863–883. [CrossRef]
79. Li, J.; Xu, L. An Adaptive Sliding-Mode Observer for Induction Motor Sensorless Speed Control. *IEEE Trans. Ind. Appl.* **2005**, *41*, 1039–1046. [CrossRef]
80. Rekha, K.; Mariaraja, P.; Kuppuswamy, A. Induction Motor Rotor Speed Observer Using Sliding-Mode Controller Based on Back EMF. *Int. J. Sci. Eng. Technol. Res.* **2014**, *3*, 3178–3182.
81. Xu, L. Sensorless field orientation control of induction machines based on a mutual MRAS scheme. *IEEE Trans. Ind. Electron.* **1998**, *45*, 824–831.
82. Benchaib, A.; Rachid, A.; Audrezet, E.; Tadjine, M. Real time sliding mode observer and control of an induction motor. *IEEE Trans. Ind. Electron.* **1999**, *46*, 128–138. [CrossRef]
83. Yazid, K.; Ibtiouen, R. Application of EKF to Parameters Estimation for Speed Sensorless and Neural Network Control of an Induction Motor. In Proceedings of the 6th WSEAS International Conference on Power Systems, Lisbon, Portugal, 22–24 September 2006; pp. 279–283.
84. Salvatore, L.S.; Stasi, L.T. A new EKF-Based Algorithm for Flux Estimation in Induction Machines. *IEEE Trans. Ind. Electron.* **1993**, *40*, 496–504. [CrossRef]
85. Picard, C.; Ranieri, F. Application of he Extended Kalman Filter to Parameter and State Estimation of Induction Motors. *Int. J. Model. Simul.* **1989**, *9*, 85–89.
86. Shi, K.L.; Chan, T.F.; Wong, Y.K.; Ho, S.L. Speed Estimation of an Induction Motor Drive Using Extended Kalman Filter. *IEEE Trans. Ind. Appl.* **2000**, 243–248.
87. Iwasaki, T.; Kataoka, T. Applications of an Extended Kalman Filter to parameter Identification of an induction motor. *IEEE Trans. Ind. Electron.* **1989**, *48*, 248–253.
88. Lin, F.-J. Robust Speed-Controlled Induction-Motor Drive Using EKF and RLS Estimators. *IEEE Proc. Electr. Power Appl.* **1996**, *143*, 186–192. [CrossRef]
89. Aquilla, A.D.; Cupertino, F.; Salvatore, L.; Stasi, S. Kalman Filter Estimators Applied to Robust Control of Induction Motor Drives. In Proceedings of the IECON'98, Aachen, Germany, 31 August–4 September 1998; pp. 2257–2262.

90. Gazafroodi, S.M.M.; Dashti, A. A Novel MRAS Based Estimator for Speed-Sensorless Induction Motor Drive. *Iran. J. Electr. Electron. Eng.* **2014**, *10*, 304–313.

91. Brandstetter, P.; Dobrovsky, M. Speed Estimation of Induction Motor Using Model Reference Adaptive System with Kalman Filter. *Theor. Appl. Electr. Eng.* **2013**, *12*, 22–28. [CrossRef]

92. Bhandri, M.M.; Patil, A.; Patil, P.; Patil, A.; Patil, R.; Patil, G. Speed Control of Three Phase Induction Motor by Using MRAS. *Int. Res. J. Eng. Technol.* **2016**, *3*, 237–242.

93. Van Der Broeck, H.W.; Skudelny, H.C.; Stanke, G.V. Analysis and Realization of a Pulse width Modulator Based on Voltage Space Vectors. *IEEE Trans. Ind. Appl.* **1998**, *24*, 142–150. [CrossRef]

94. Comanescu, M.; Xu, L. Sliding mode MRAS speed estimators for sensorless vector control of induction machine. *IEEE Trans. Ind. Electron.* **2006**, *53*, 146–153. [CrossRef]

95. Brahim, L.; Tadakuma, S.; Akdag, A. Speed control of induction motor without rotational transducers. *IEEE Trans. Ind. Appl.* **1999**, *35*, 844–850. [CrossRef]

96. Karanayil, B.; Rahman, M. Grantham an implementation of a programmable cascaded low-pass filter for a rotor flux synthesizer for an induction motor drive. *IEEE Trans. Power Electron.* **2004**, *19*, 257–263. [CrossRef]

97. Rashed, M.; Stronac, A. A stable back-EMF MRAS-based sensorless low speed induction motor drive insensitive to stator resistance variation. *IEEE Proc. Electr. Power Appl.* **2004**, *151*, 685–693. [CrossRef]

98. Maiti, S.; Chakraborty, C. A new instantaneous reactive power based MRAS for sensorless induction motor drive. *Simul. Model. Pract. Theory* **2010**, *18*, 1314–1326. [CrossRef]

99. Li, Z.; Xu, L. A Mutual MRAS Identification Scheme for Position Sensorless Field Orientation Control of Induction Machines. In Proceedings of the 13th IAS Annual Meeting, Orlando, FL, USA, 8–12 October1995; pp. 159–165.

100. Shin, M.H.; Hyun, D.S.; Cho, S.B.; Choe, S.Y. An Improve Stator Flux Estimation for Speed Sensorless Stator Flux Orientation Control of Induction Motors. *IEEE Trans. Power Electron.* **2000**, *15*, 312–318. [CrossRef]

101. Park, C.W.; Kwon, W.H. Simple and robust speed sensorless vector control of induction motor using stator current based MRAC. *Electr. Power Syst. Res.* **2004**, *71*, 257–266. [CrossRef]

102. Abraham, L.A.; Arunchand, K.; Reddy, S. An Artificial Intelligence Based Induction Motor Speed control and Estimation using conventional MRAS with dynamic reference modal. *Int. J. Eng. Res. Appl.* **2012**, *2*, 87–92.

103. Karanayil, B.; Rahman, M.F.; Grantham, C. Online Stator and Rotor Resistance Estimation Scheme Using Artificial Neural Networks for Vector Controlled Speed SensorlessInduction Motor Drive. *IEEE Trans. Ind. Electron.* **2007**, *54*, 167–176. [CrossRef]

104. Venkadesan, A.; Himavathi, S.; Sedhuraman, K.; Muthuramalingam, A. Design and field programmable gate array implementation of cascade neural network based flux estimator for speed estimation in induction motor drives. *IET Electric Power Appl.* **2017**, *11*, 121–131. [CrossRef]